haematologica
Journal of the Ferrata Storti Foundation

Independent prognostic value of semaphorin-4D, interleukin-1β and complement activation in newly diagnosed multiple myeloma patients

by Ioannis Ntanasis-Stathopoulos, Panagiota-Efstathia Nikolaou, Charalampos Filippatos, Marios Miliotis, Ioannis V. Kostopoulos, Panagiotis Bakouros, Manousos Makridakis, Christine-Ivy Liacos, Konstantinos Nikolopoulos, Stamatia Laidou, Anastasia Chatzidimitriou, Maria Frantzi, Efstathios Kastritis, Despina Fotiou, Maria Gavriatopoulou, Antonia Vlahou, Artemis G. Hatzigeorgiou, Ourania Tsitsilonis, Meletios Athanasios Dimopoulos and Evangelos Terpos

Received: May 13, 2026.
Accepted: August 20, 2026.

Citation: Ioannis Ntanasis-Stathopoulos, Panagiota-Efstathia Nikolaou, Charalampos Filippatos, Marios Miliotis, Ioannis V. Kostopoulos, Panagiotis Bakouros, Manousos Makridakis, Christine-Ivy Liacos, Konstantinos Nikolopoulos, Stamatia Laidou, Anastasia Chatzidimitriou, Maria Frantzi, Efstathios Kastritis, Despina Fotiou, Maria Gavriatopoulou, Antonia Vlahou, Artemis G. Hatzigeorgiou, Ourania Tsitsilonis, Meletios Athanasios Dimopoulos and Evangelos Terpos. Independent prognostic value of semaphorin-4D, interleukin-1β and complement activation in newly diagnosed multiple myeloma patients. Haematologica. 2026 Sept 3. doi: 10.3324/haematol.2026.301208 [Epub ahead of print]

Publisher's Disclaimer.
E-publishing ahead of print is increasingly important for the rapid dissemination of science. Haematologica is, therefore, E-publishing PDF files of an early version of manuscripts that have completed a regular peer review and have been accepted for publication.
E-publishing of this PDF file has been approved by the authors.
After having E-published Ahead of Print, manuscripts will then undergo technical and English editing, typesetting, proof correction and be presented for the authors' final approval, the final version of the manuscript will then appear in a regular issue of the journal.
All legal disclaimers that apply to the journal also pertain to this production process.

Independent prognostic value of semaphorin-4D, interleukin-1β and complement activation in newly diagnosed multiple myeloma patients

Ioannis Ntanasis-Stathopoulos*[1], Panagiota-Efstathia Nikolaou*[1,2], Charalampos Filippatos[1], Marios Miliotis[3], Ioannis V Kostopoulos[4], Panagiotis Bakouros[4], Manousos Makridakis[5], Christine-Ivy Liacos[1], Konstantinos Nikolopoulos[2], Stamatia Laidou[6], Anastasia Chatzidimitriou[6,7], Maria Frantzi[8], Efstathios Kastritis[1], Despina Fotiou[9], Maria Gavriatopoulou[1], Antonia Vlahou[5], Artemis G Hatzigeorgiou[3], Ourania Tsitsilonis[4], Meletios Athanasios Dimopoulos[1,10], Evangelos Terpos[1#].

(1) Department of Clinical Therapeutics, Alexandra Hospital, School of Medicine, National and Kapodistrian University of Athens, Athens, Greece

(2) Laboratory of Pharmacology, Faculty of Pharmacy, National and Kapodistrian University of Athens, Athens, Greece

(3) DIANA-Lab, Department of Computer Science and Biomedical Informatics, University of Thessaly, Lamia, Greece

(4) Section of Animal and Human Physiology, Department of Biology, National and Kapodistrian University of Athens, Athens, Greece

(5) Laboratory of Biotechnology, Academy of Athens Biomedical Research Foundation, Athens, Greece

(6) Institute of Applied Biosciences, Centre for Research and Technology Hellas, Thessaloniki, Greece.

(7) Department of Molecular Medicine and Surgery, Karolinska Institutet, Stockholm, Sweden.

(8) Department of Biomarker Research, Mosaiques diagnostics GmbH, 30659 Hannover, Germany

(9) Department and Laboratory of Pathophysiology, Medical School, National and Kapodistrian University of Athens, Athens, Greece

(10) Department of Medicine, Korea University, Seoul, South Korea

#Address of correspondence: Professor Evangelos Terpos, Department of Clinical Therapeutics, Alexandra Hospital, School of Medicine, National and Kapodistrian University of Athens, 80 Vas. Sophias Ave, 11528 Athens, Greece; email: eterpos@med.uoa.gr; tel: +302132162846

*The authors have equally contributed to this work

Key words: multiple myeloma; biomarker discovery; semaphorin-4D; IL-1β; complement

Short title: Complement and IL-1β as prognostic biomarkers in multiple myeloma

Acknowledgments

The study was funded by the International Myeloma Society Translational Research Award to Professor E. Terpos, Project Title: “Comprehensive exploration of molecular

pathways and biomarkers in myeloma-induced bone disease: a multi-omics approach for personalized therapeutic management", Funding Cycle: 2024-2025.

Author Contributions

INS was responsible for designing the protocol, writing the protocol, collecting patient data, conducting the search and writing the manuscript. PEN designed the experimental protocol, conducted research and analyses in plasma (all techniques), analyzed ELISA and proteomics data, interpreted the results and wrote the original draft of the manuscript. CF was responsible for extracting and analyzing data and performing data analysis. MMi conducted genomic data analysis and visualization. IVK conducted multiplex analysis. PB retrieved patient bone marrow samples and conducted cell sorting. MMa conducted proteomic analysis in plasma. CIL retrieved, anonymized and organized patient samples and secured paired plasma samples from progressors. MF performed acquisition of plasma proteomics and reviewed the manuscript. SL and AC conducted genomic analyses. KN conducted the ELISA experiments, genomic DNA extraction and reviewed the manuscript. MG, EK and DF recruited and monitored patients, supervised clinical protocols, wrote the clinical protocol and reviewed the manuscript. AV supervised proteomic analyses and reviewed the manuscript. AGH supervised genomic analyses of the data and reviewed the manuscript. OT designed the protocol, retrieved bone marrow patient samples, supervised flow cytometry experiments unit and reviewed the manuscript. MAD supervised the work and reviewed the manuscript. ET designed the protocol, supervised and guided the work, was responsible for the provision of adequate

funding for all conducted research, organized the coordination and communication across authors and revised the manuscript.

Competing Interests

No competing interests to report

Data Availability Statement

All patient related data are available upon request from the corresponding author, and the raw data of the proteomic analysis are available on MassIVE (Mass Spectrometry Interactive Virtual Environment) open access repository with the Dataset Identifier: MSV000101409. The password for reviewing purposes is BoneDisease. (Upon publication data will also be available at ProteomeXchange with identifier: PXD076747).

Abstract

Multiple myeloma represents a systemic disease of the bone marrow (BM) niche, in which immune and skeletal pathways are tightly interconnected. However, the independent prognostic significance of bone and immune-related markers in newly diagnosed multiple myeloma (NDMM) remains incompletely understood.

Semaphorin (Sema) 4D, activin-A, and periostin ELISA, LEGENDplex™ Human Bone Metabolism Panel and proteomic analysis for novel biomarker identification were conducted in 71 consecutive samples from NDMM patients. In 25 patients, genomic analysis was performed on sorted clonal plasma cells.

NDMM patients had a median age at diagnosis of 65 years and a median follow-up of 2.5 years. Interleukin (IL)-1β and Sema4D levels predicted progression-free survival (PFS), highlighting their role in disease relapse. Proteomic profiling revealed a systemic signature associated with worse prognosis, enriched in complement activation components. Complement C5 significantly affected PFS and time to progression (TTP). IL-1β and C5 predicted PFS independently of the second revision of the International Staging System (R2-ISS) stage, and a similar trend was noted for Sema4D. Myeloma bone disease (MBD) did not significantly affect overall survival, PFS, or TTP, suggesting that contemporary treatments mitigate its impact. Genomic analyses identified variants associated with inferior PFS, including HLA-DRB5 (c.300_306delinsCGGG) and HLA-DQB1 (c.317_319delinsCGG).

Sema4D and the IL-1β–complement cascade emerged as key drivers of disease progression, independent of R2-ISS stage, representing potential prognostic and therapeutic targets in NDMM.

Introduction

Multiple Myeloma (MM) is a complex hematological malignancy characterized by the clonal proliferation of malignant plasma cells within the bone marrow (BM).[1] MM is driven by interactions between tumor cells and their surrounding niche, the bone marrow microenvironment (BMME), which consists of a heterogeneous network of stromal cells, immune cell populations, cytokines, and extracellular matrix components.[2,3] This environment represents a functional interface between the immune system and bone remodeling processes, highlighting the tight coupling between immune regulation and bone metabolism in MM.[4,5]

Complex interactions between myeloma plasma cells and the BMME lead to the disruption of normal bone remodeling.[6] Dysregulated bone remodeling can be affected by a pro-inflammatory milieu, as myeloma cells and stromal components secrete a wide range of cytokines, including interleukin (IL)-1β, IL-6, tumor necrosis factor (TNF)-α, and other osteoclast-activating factors, that simultaneously promote plasma cell growth, immune dysregulation, and bone destruction[7,8]. Proteomic studies in MM have identified extensive alterations in BM proteins involved related to immune regulation, inflammation, coagulation, and bone metabolism.[9–11] Mass spectrometry–based analyses of BM interstitial fluid have revealed proteomic signatures associated with clinical outcomes.[12,13] Among these, molecules involved in immune modulation and inflammation, such as ILs[14,15] and components of the complement cascade[16], are particularly interesting due to their dual role in regulating plasma cells–microenvironment interactions and bone homeostasis. For example, IL-6 acts as a key growth and survival factor for immature plasma cells while preventing

terminal differentiation, thereby sustaining the malignant phenotype.[17] At the same time, the secretion of IL-6 by osteoclasts enhances the proliferation of myeloma cells but also promotes bone resorption through the upregulation of RANKL.[2,18] This interplay exemplifies a vicious cycle of bone destruction and tumor expansion expanding the concept of osteoimmunology, where immune signaling and bone metabolism are interconnected.[18,19] However, the independent prognostic significance of bone and immune related markers in newly diagnosed MM patients (NDMM) remains incompletely understood.

The primary aim of this study was to investigate the association of skeletal and immune-related biomarkers, including semaphorin-4D (SEMA4D), activin-A, periostin, and an established panel of bone metabolism with clinical outcomes, namely overall survival (OS), progression-free survival (PFS), and time to progression (TTP). We also employed high-though put mass-spectrometry based plasma proteomic profiling in order to identify novel circulating biomarkers and molecular mechanisms that determine disease outcomes. Since in the BM microenvironment these markers could also reflect bone turnover, we examined their impact on discriminating underlying myeloma bone disease (MBD) and imaging-defined osteolytic lesions. While BM-derived specimens may directly reflect the microenvironment, plasma offers a minimally invasive and clinically accessible source for biomarker discovery.[20,21] Therefore, in our study we selected plasma proteomics over BM to enable future translation into routine clinical practice. Furthermore, we evaluated the impact of MBD on OS, PFS and TTP in patients with NDMM, in the context of contemporary anti-myeloma therapies. Finally, whole exome sequencing (WES) of clonal and non-clonal

BM cells was conducted to identify genetic variants associated with clinical outcomes and provide an integrative view of the molecular determinants of disease progression.

Methods

Detailed methodology is described in the supplementary file.

Study population and sample collection

Data and plasma samples from sequential 71 patients with NDMM (***Supplementary Table 1***) were analyzed with ELISA, a bone metabolism protein panel and mass-spectrometry based proteomics. ELISA assays were also applied in n= 21 paired plasma samples obtained at the prior smoldering multiple myeloma (SMM) or monoclonal gammopathy of undetermined significance (MGUS) stage from the same patients and plasma samples from n=25 independent, sex and aged matched SMM/MGUS patients to investigate bone-related biomarkers at earlier disease stages.

All patients provided written informed consent for the use of their biological material and clinical data, including secondary research analyses where applicable. The study was reviewed and approved by the Institutional Review Board (173/2024, 07/06/2024, NKUA). Patient identifiers were removed prior to the analysis to ensure confidentiality and compliance with the General Data Protection Regulation (GDPR) and the Health Insurance Portability and Accountability Act (HIPAA).

Plasma measurements

Plasma concentrations of SEMA4D, activin-A, and periostin were quantified using commercially available sandwich ELISA kits (Human SEMA4D ELISA Kit, Cat. No. LS-F22167-1; Human Activin A ELISA Kit, Cat. No. LS-F54506-1; Periostin ELISA Sandwich

Kit, Cat. No. LS-F3645; all from LSBio, Shirley, MA), according to the manufacturers' instructions. To quantify additional circulating markers related to bone metabolism and inflammation using the LEGENDplex™ Human Bone Metabolism Panel (13-plex; BioLegend, San Diego, CA, USA), a multiplex bead-based immunoassay. The panel allows the simultaneous quantification of 13 proteins, including cytokines and bone-related mediators, in small plasma volumes. Plasma samples were collected and processed for proteomic analysis. The filter aided sample preparation (FASP) was performed as we have previously reported.[22–24] All LC-MS/MS experiments were conducted using the Dionex Ultimate 3000 UHPLC system coupled with the high-resolution nano-ESI Q-Ex active Plus - Orbitrap mass spectrometer (Thermo Scientific, Waltham, MA). False discovery rate (FDR) validation was based on q value: target FDR : 0.01[25]. Quantification was performed at the peptide level employing a clustering approach as previously described.[26,27] Differential protein expression analysis was performed using the ProtE R package.[28] Pathway enrichment analysis of proteins of interest was conducted using the web-based GEne SeT AnaLysis Toolkit (WebGestalt).[29,30]

Genomics

Clonal plasma cells and non-clonal BM populations were sorted from a sub-cohort of n=25 NDMM patients. Flow cytometry and cell sorting were performed on a BD FACSMelody™ (BD Biosciences). Total DNA was isolated from sorted cell samples using the NucleoSpin® TriPrep kit (Macherey-Nagel, Germany) following the manufacturer's protocol. Whole-exome sequencing (WES) was performed. Library preparation and whole exome enrichment were performed using the Twist Library Preparation EF Kit

and the Twist Target Enrichment Standard Hybridization v2 Protocol (Twist Bioscience, USA) following the manufacturer's instructions. Sequencing was performed on the Illumina NextSeq 2000 platform (Illumina, San Diego, CA, USA) to generate 150 bp paired-end reads, achieving a mean coverage depth of 90X. Sequencing reads underwent quality control with FastQC, to assess base quality, GC content and adapter contamination. Reads were aligned to human genome assembly GRCh37 using the DRAGEN Enrichment App (Illumina, USA), which also performed variant calling for single nucleotide variants (SNVs) and small insertions/deletions. Variant annotation and filtering were performed using ANNOVAR tool with population (e.g., gnomAD) and clinical (e.g., ClinVar) databases and Franklin database to prioritize variants based on frequency and pathogenicity for downstream interpretation.

Statistical analysis

Mann-Whitney U test or Kruskal-Wallis test were applied to the non-normally distributed data. Categorical variables were compared using Fisher's exact test or the Chi-square test, as appropriate. To evaluate the prognostic value of individual protein expression levels with respect to clinical outcomes—OS, PFS, and TTP—survival analysis was performed. Survival curves were compared between groups with low and high protein expression defined by the maximally ranked statistics-derived cutoff and the Kaplan Meier method, and statistical significance was assessed via the log-rank test. To estimate the association between protein expression and the risk of an event, univariate survival analysis was performed using Cox proportional hazards models. Protein expression was included as an independent variable, categorized according to the optimal cutoffs, while time-to-event and event status were defined as dependent

variables. Prior to model fitting, the proportional hazards assumption was verified for all variables using Schoenfeld residuals. For each model, the hazard ratio (HR), 95% confidence interval (95% CI), and p-value were calculated. To identify proteins independently associated with clinical outcomes, multivariate Cox models were subsequently adjusted for key clinical confounders, including age (< or ≥65 years), sex, induction treatment, and autologous stem-cell transplantation (ASCT). Finally, an exploratory multivariable Cox model was constructed incorporating multiple significant biomarkers simultaneously to assess their joint prognostic utility. To control for type I errors across all multiple comparisons, p-values were adjusted using the Benjamini-Hochberg FDR method. A p-value of <0.05 is considered statistically significant across this study. This analytical framework was applied to circulating biomarkers quantified by ELISA, LEGENDplex, and proteomics.

Results

SEMA4D and periostin are increased in patients who progress to MM regardless of the presence of MBD

Given their established roles in bone remodelling and tumour–bone interactions, circulating levels of Semaphorin 4D (SEMA4D), periostin, and activin-A were assessed across the stages of MM progression. MGUS/SMM non-progressor patients (n=25) were compared with MGUS/SMM patients who progressed to MM (n = 21). SEMA4D and periostin levels were significantly higher in MGUS/SMM patients who progressed to MM compared with those who did not show disease progression regardless of the presence of MBD (***Figures 1A and 1B***). Statistically significantly increased levels of SEMA4D and periostin were also observed in patients with NDMM compared with

non-progressors. No difference was observed between MGUS/SMM or MM patients with and without MBD (***Figure 1A and 1B***). Activin-A levels were similar between non-progressors and MM progressors either at the MGUS/SMM state or at the timepoint of MM diagnosis with and without MBD (***Figure 1C)***. None of these markers showed a significant association with performance status (PS) or the number of osteolytic lesions (data not shown).

SEMA4D is increased in NDMM patients and is predictive of disease progression

The increased levels of SEMA4D and periostin in NDMM patients, were further associated with clinical outcomes (***Supplementary Table 2***). Importantly, in NDMM patients, SEMA4D predicted PFS and TTP (***Figures 2A and 2B***) and remained a prognostic marker for PFS in the multivariate adjusted Cox model, with a trend towards predicting TTP (adjusted HR-aHR = 3.03, 95% CI: 1.06–8.66, p = 0.03, and aHR = 3.62, 95% CI: 0.98–13.29, p = 0.05, respectively), highlighting its potential role as both a prognostic biomarker and a therapeutic target. Although periostin was significantly associated with OS in univariate analysis (***Supplementary Figure 1***) (HR = 6.02, 95% CI: 1.60–22.66; p adjusted for multiple comparisons = 0.048), this association was not maintained in multivariate analysis, suggesting that its prognostic value may be influenced by additional factors.

Markers of bone metabolism and cytokines are not significantly different in patients with and without MBD

To comprehensively assess alterations in bone metabolism–related signaling, circulating levels of key regulators of osteoclast and osteoblast activity—OPG, OPN, PDGF-BB, ALPL, ACP5, leptin, RANKL (TRANCE), TNF-α, IL-6, PTH, IL-1β, BMP-2, and

DKK-1—were quantified using the LEGENDplex™ Human Bone Metabolism Panel **(*Supplementary Figure 2)***. The markers were initially compared between NDMM patients with and without MBD. Mann–Whitney U analysis revealed that only DKK-1 levels showed a trend towards increased levels in MBD status (p = 0.062), which were not significant after adjustment for multiple comparisons (adjusted p = 0.401) (***Supplementary Figure 3***). No statistically significant differences were observed for the remaining bone metabolism markers (***Supplementary Table 3***).

Subsequently, the association between circulating markers of bone metabolism and the presence of osteolytic lesions was examined. No statistically significant differences were identified after correction for multiple testing. OPG levels tended to differ according to the presence of osteolytic lesions (p = 0.078; adjusted p = 0.796). (***Supplementary Table 4***).

IL-1β circulating levels are predictive of progression free survival and osteopontin predicts overall survival

Bone metabolism protein analysis with the multiplex bead-based flow assay showed that at NDMM, IL-1β predicted PFS (aHR: 5.55, 95%CI: 1.14-27.03, p = 0.03), thus inflammation remains a key pathophysiological mechanism in MM that could be targeted by emerging therapies (***Figure 3A and Supplementary Table 2***). OPG predicted OS (aHR: 10.82, 95%CI: 1.29 - 90.65, p = 0.02) (***Figure 3B***), indicating that bone turnover remains important for survival outcomes; however, the small number of cases analysed limits our interpretation.

Plasma proteome reveals novel biomarkers of disease state and progression

Circulating proteomic profiling revealed a distinct systemic signature associated with MBD, extending beyond conventional markers of bone turnover. Patients with MBD exhibited upregulation of proteins linked to tumor burden and immune activation (B2M, L1TD1), cytoskeletal remodelling and cell motility (SHTN1, MYH16, FHOD1), and endothelial, coagulation, and inflammatory pathways (F12, AMBP, ARAP3), consistent with an actively remodelled BM niche. In contrast, downregulation of stress-response and vesicular trafficking proteins (HSPA1, ARFGEF3) suggests exhaustion or rewiring of protective homeostatic mechanisms in MBD, potentially amplifying inflammatory signalling and tissue damage (***Figure 4 and Supplementary Table 5)***. L1TD1 seems the most promising candidate, since it has been described as a tumor progressor marker in malignant conditions,[31,32] and had the lowest p value upon FDR adjustments.

Thirty-four circulating proteins were initially associated with the presence of osteolytic lesions, although none remained significant after correction for multiple testing. Pathway enrichment analysis of these proteins highlighted post-translational protein phosphorylation, regulation of insulin-like growth factor (IGF) transport and uptake by IGF-binding proteins, platelet activation and degranulation, and complement-related pathways, including regulation of the complement cascade and activation of C3 and C5. Collectively, these findings point to a coordinated activation of complement-, platelet-, and IGF-associated signalling in patients with osteolytic lesions, despite the lack of statistical significance after adjustments (***Supplementary Figure 4***).

Subsequently, an analysis was performed to identify proteins that commonly defined all three major outcome-related parameters based on multivariate analysis. A common protein signature was identified across all endpoints (i.e., OS, PFS and TTP)

that comprised of 13 proteins, namely IGKV2-30, CFP, MASP1, F9, CLEC3B, ATRN, FGB, BCHE, ITIH4, C5, CPN1, LRG1, and PLG using Venn diagrams **(*Figure 5A*)**. Pathway enrichment analysis revealed that these proteins are predominantly clustered within complement activation, platelet function, and hemostatic pathways. Specifically, significant enrichment was observed in the complement cascade, including initial triggering of complement, activation of C3 and C5 and regulation of the complement cascade, highlighting the coordinated activation of innate immune mechanisms (***Figure 5B***). Association of proteomic findings with OS was performed but the estimates were characterized by wide confidence intervals and instability, limiting their interpretability. This likely reflects the limited number of events and/or insufficient follow-up duration. However, PFS and TTP estimates were reliable. Indicatively, using an optimal cutoff value of 281.44 for C5, elevated levels were significantly associated with inferior clinical outcomes in NDMM patients. In multivariate Cox regression analysis, high C5 levels remained an independent predictor of shorter PFS (aHR = 4.13, 95% CI: 1.12–15.27, p = 0.033). Similarly, elevated C5 was independently associated with shorter TTP (aHR = 7.89, 95% CI: 1.02–61.23, p = 0.048) *(**Figure 6A and 6B**)*.

IL-1β and C5 predict progression free survival independently of disease stage, while SEMA4D remains prognostic

To assess whether inflammatory and complement-related biomarkers provide prognostic information independent of established clinical factors, a multivariate Cox proportional hazards model was constructed including age, sex, treatment, ASCT, the second revision of the International Staging System (R2-ISS) stage, and the biomarkers SEMA4D, C5, and IL-1β. In this model, both C5 and IL-1β retained independent

prognostic significance for PFS. Specifically, elevated C5 levels were associated with a markedly increased risk of progression (aHR = 38.19, 95% CI: 1.47–994.27, p = 0.028), while IL-1β also independently predicted inferior PFS (aHR = 49.19, 95% CI: 2.29–1056.31, p = 0.013). In contrast, SEMA4D showed a trend toward significance (aHR = 7.17, 95% CI: 0.74–69.13, p = 0.088), suggesting a potential but less robust independent effect. Interestingly, R2-ISS stage was not significantly associated with PFS in the multivariate model (aHR = 2.36, 95% CI: 0.56–9.87, p = 0.239), supporting the notion that these biomarkers have a potential prognostic value beyond R2-ISS.

MBD presence at diagnosis does not impact on patient characteristics and clinical outcome

NDMM patients had a median age at diagnosis of 65 years (range 46–89) and median follow-up duration was 2.5 years (range 1.7–3.4); 39 (54.9%) were women, and 46 (64.8%) presented with MBD. ***Supplementary Table 1*** summarizes the baseline characteristics of patients at the time of diagnosis, stratified according to the presence or absence of MBD. No statistically significant differences were observed between the two groups, with the exception of disease stage according to the ISS, and risk stratification according to the R2-ISS. Notably, almost half of the patients with MBD were diagnosed with more than ten osteolytic lesions (19 of 46 patients, 41.3%).

Patients with MBD did not show statistically significant differences in OS (1.29, 95%CI: 0.34-4.85, p=0.710), PFS (0.79, 95%CI: 0.36-1.74, p=0.559), or TTP (0.68, 95%CI: 0.28-1.69, p=0.410) compared to those without MBD, suggesting that current anti-myeloma treatments mitigated the impact of MBD on patient outcomes (***Figures 7, 8A and 8B***).

Exploratory genomic landscape and association with clinical outcomes

WES was performed in paired clonal and bulk BM cells from 25 patients with NDMM to investigate associations between genomic variants and clinical phenotypes. No variants were significantly associated with MBD or the number of osteolytic lesions per patient after FDR correction.

Following adjustment for multiple testing, OS analysis identified two variants significantly associated with outcome. These included a synonymous exonic variant in *MUC22* (c.4296T>C) classified as possibly benign and non-somatic, and a non-synonymous exonic variant in *GCNT1* (c.1103C>T) classified as possibly benign and identified as somatic. Both variants remained significantly associated with OS after adjustment, despite their predicted low functional impact (***Supplementary Figures 5A and 5B***). Given that TTP and PFS were identical in this subcohort, subsequent analyses focused on variants associated with inferior TTP. The strongest associations were observed for variants in HLA class II genes, including a non-frameshift exonic variant in *HLA-DRB5* (c.300_306delinsCGGG) classified as possibly pathogenic and non-somatic, and a non-synonymous exonic variant in *HLA-DQB1* (c.317_319delinsCGG) of uncertain significance identified as somatic (***Supplementary Figures 5C and 5D***). In addition, inferior TTP was associated with a synonymous exonic variant in *NPIPB11* (c.1659G>C) classified as likely benign and non-somatic, as well as a non-synonymous exonic variant in *OR2T8* (c.152_154delinsGCA) of uncertain significance identified as somatic (***Supplementary Figures 5E and 5F***).

Discussion

The present study investigates the clinical and molecular parameters of MM progression and MBD utilizing targeted ELISA, a multiplex bone metabolism protein

assay, and an untargeted proteomic approach. At molecular level, circulating biomarkers—specifically periostin and SEMA4D—showed prognostic value, as their levels significantly increased in patients who progressed from MGUS/SMM to MM compared with non-progressors, irrespective of the presence of MBD. Furthermore, SEMA4D demonstrated prognostic significance for PFS in NDMM patients, in parallel with IL-1β, as revealed in the bone metabolism assay. Proteomic analysis identified multiple proteins that significantly influenced patient outcomes with respect to TTP and PFS. The association of these proteins with immune-related molecular pathways, highlighted the involvement of the complement system in MM progression, with complement component C5 emerging as a potential prognostic and potential therapeutic target. Our findings demonstrate that the presence of MBD in NDMM patients does not affect survival or disease progression, suggesting that bone involvement at diagnosis does not translate into worse clinical outcomes, at least within the studied population and in the frame of this specific therapeutic context. In a subcohort of patients, genomic profiling of clonal plasma cells identified HLA variants associated with lower disease progression rates, but no association with MBD was observed.

In a previous study, we have identified biomarkers associated with serum calcium levels, increased bone resorption and ISS, like SEMA4D. There was a trend for higher SEMA4D levels in patients with osteolysis, while patients with a diffuse MRI pattern had higher BM SEMA4D levels.[33] Moreover, in another study, we found that periostin correlated with the presence of fractures (indicating MBD) and a diffuse MRI pattern of BM infiltration.[34] Concerning circulating biomarkers, we have previously shown that activin-A was associated with increased bone resorption and extensive myeloma bone

disease (MBD) as well as with inferior survival.[35] In this context, we initially aimed to validate these circulating markers in patients with NDMM, with and without MBD, not only at diagnosis but also using paired samples from the same individuals who progressed from the asymptomatic SMM/MGUS stage to overt MM. Regarding biomarker evaluation, among SEMA4D, activin-A, and periostin, only SEMA4D demonstrated a prognostic value at the NDMM stage, showing a statistically significant association with PFS in NDMM patients. Semaphorins are signaling molecules involved in osteoclast–osteoblast communication, with SEMA4D exerting a dominant inhibitory effect on osteoblast differentiation and regulating osteoblast motility.[36,37] Previous studies have initially demonstrated elevated levels of SEMA4D and its receptor Plexin-B1 levels in both serum and BM plasma of patients with active MM.[38] Our findings align with the disrupted bone metabolism in MM, marked by reduced osteoblast activity.[39] MM cells appear to inhibit osteoblast differentiation through a SEMA4D-mediated mechanism[40]. Additionally, elevated SEMA4D levels in the BM microenvironment may also derive from osteocytes, besides SEMA4D production by osteoclasts.[41]

A novel finding of our study is that increased plasma levels of IL-1β are associated with inferior PFS. IL-1β is highly produced in almost all plasma cells of MM patients, whereas it is largely absent in normal plasma cells.[42] This cytokine plays a central role in the BM microenvironment by stimulating stromal cells to produce IL-6, a key survival factor for myeloma cells, by promoting osteoclast activity driving bone resorption, and by contributing to the development of osteolytic lesions.[43] Experimental evidence indicates that SEMA4D can regulate cytokine networks including IL-1β production in immune contexts, with SEMA4D knockout mice showing

reduced IL-1β expression in response to inflammatory stimuli.[44] This evidence highlights the importance of the SEMA4D-IL-1β axis as a novel finding driving disease progression, as shown in our study.

Extensive proteomic analysis in the whole patient cohort revealed that MBD has a limited impact on the plasma proteome. Only L1TD1, a protein related to stemness, tended to maintain its high statistical significance between patients with and without MBD. The identification of CFP (properdin), MASP1, and C5 among proteins associated with adverse outcomes highlights a sustained activation of the complement system through both the alternative and lectin pathways. Convergence on C5 suggests amplification of downstream inflammatory signalling via C5a generation and membrane attack complex formation, potentially linking innate immune activation to BM damage and disease progression.[45] This finding reinforces the central involvement of innate immunity and the complement system in MM pathobiology, and underlines potential diagnostic and therapeutic applications. The complement system is an integral component of innate immunity and contributes to tissue homeostasis and skeletal regeneration. Complement proteins play critical roles not only in immune activation but also in bone development and bone tissue homeostasis, influencing osteoblast and osteoclast differentiation, metabolism, and intercellular communication.[46] To date, limited studies have examined how innate immunity mediating MM progression and MBD. Although there is no direct association between the pathophysiology of MM and PNH, existing complement inhibitors used in and paroxysmal nocturnal hemoglobinuria (PNH)[47] could potentially be repurposed for MM in the future.

Importantly, in our multivariate analysis including ISS stage and established clinical covariates, both IL-1β and C5 retained independent prognostic significance for PFS, indicating that their impact is not merely a reflection of disease burden. Notably, R2-ISS stage did show statistical significance in this model, suggesting that these biomarkers capture a distinct biological dimension related to inflammation and innate immune activation that is not encompassed by conventional staging systems. Collectively, these findings support the existence of an inflammation-driven high-risk phenotype in MM, independent of tumor load, with potential implications for risk stratification and therapeutic targeting.

Consistent with recent studies[48,49], MBD defined by modern imaging techniques (mainly whole body low dose computed tomography) does not appear to directly affect survival but rather impacts patients' quality of life. In our cohort of 71 NDMM patients, treated with contemporary MM therapies—including proteasome inhibitors, immunomodulatory drugs and anti-CD38 monoclonal antibodies—MBD did not influence survival outcomes. This observation is further supported by the absence of the MBD status in the current MM staging systems. We propose that future studies should include larger cohorts to enable stratification based on treatment modalities, thus allowing the assessment of whether different therapeutic strategies exert differential effects on the prognostic impact of MBD.

The HLA associations observed in our study, including variants in HLA-DRB5 and HLA-DQB1 alleles, are consistent with previous GWAS data, highlighting the HLA region as a key risk locus for mature B-cell-derived malignancies.[50,51] Epidemiological analysis in MM, further demonstrates the protective and predisposing effects of specific HLA

alleles and haplotypes: HLA-B*44* and *A*02-B*44-DRB1*04 haplotypes were associated with reduced MM risk, whereas HLA-B*07* and *A*02-B*07-DRB1*04 conferred increased susceptibility.[52] Presentation of altered self-antigens by HLA molecules present on B cells to T cell receptors could stimulate autoantibody production, suggesting a mechanism by which HLA variation may influence disease susceptibility. Importantly, in the context of our findings, there is no direct evidence linking these HLA variants with SEMA4D or IL-1β, although the observed variants may contribute indirectly to immune modulation within the tumor microenvironment.

This study has several limitations that should be considered when interpreting the findings. First, the relatively limited sample size, particularly within the genomic subgroup analysis cohort, may have reduced statistical power to detect more subtle associations and increased the risk of type II error. Second, the median follow-up duration may be insufficient to fully capture long-term outcomes, particularly OS. As MM is characterized by prolonged disease trajectories in the era of modern therapies, longer follow-up is required to confirm the robustness and durability of the observed prognostic associations. Importantly, because in our patient cohort MM was diagnosed prior to the establishment of contemporary genomic risk stratification frameworks, we were unable to comprehensively apply the most recent high-risk MM criteria, such as those proposed by the Chromosomal Genomic Stratification (CGS) model. Specifically, key genomic variables were not systematically available for all patients. This limitation may have led to incomplete adjustment for high-risk genetic features and could affect the interpretation of the independence of the investigated biomarkers from established genomic risk. Furthermore, the divergent biological roles and dynamic regulation of the investigated biomarkers (Sema4D, IL-1β, and

complement components) across different disease states and microenvironmental contexts may introduce variability that is not fully captured in a single time-point measurement. Serial assessments could provide more accurate insights into their prognostic relevance. Finally, although our findings suggest a potential prognostic role for these proteogenomic markers, external validation in an independent, well-characterized cohort is essential to confirm their generalizability and clinical utility. Future studies integrating comprehensive genomic profiling and longitudinal biomarker assessment, and standardized treatment approaches will be critical to further elucidate the role of these pathways in MM prognosis.

In conclusion, this study highlights the clinical relevance of specific plasma biomarkers including SEMA4D and IL-1β, and of the activation of the complement cascade, which could eventually help to stratify MM patients at high risk for progression. Integration of these biomarkers into multivariate prognostic models may support personalized disease management and may guide intervention strategies in MM, while also identifying sterile inflammation and the complement system as promising future therapeutic targets to mitigate disease progression.

References

1. Terpos E, Ntanasis-Stathopoulos I, Gavriatopoulou M, Dimopoulos MA. Pathogenesis of bone disease in multiple myeloma: from bench to bedside. Blood Cancer J. 2018;8(1):7.

2. Fotiou D, Katodritou E. From biology to clinical practice: the bone marrow microenvironment in multiple myeloma. J Clin Med. 2025;14(2):327.

3. Choustoulaki A, Ben-Aicha S, Fotiou D, et al. B Cells at the crossroads of cardiovascular and hematologic disease: paving the way for novel immunomodulatory therapies. Cell Physiol Biochem. 2025;59(S3):22-51.

4. Terpos E, Ntanasis-Stathopoulos I. Controversies in the use of new bone-modifying therapies in multiple myeloma. Br J Haematol. 2021;193(6):1034-1043.

5. Marino S, Petrusca DN, Roodman GD. Therapeutic targets in myeloma bone disease. Br J Pharmacol. 2021;178(9):1907-1922.

6. Terpos E, Ntanasis-Stathopoulos I, Dimopoulos MA. Myeloma bone disease: from biology findings to treatment approaches. Blood. 2019;133(14):1534-1539.

7. Mukkamalla SKR, Malipeddi D. Myeloma bone disease: a comprehensive review. Int J Mol Sci. 2021;22(12):6208.

8. Tsirkinidis P, Terpos E, Boutsikas G, et al. Bone metabolism markers and angiogenic cytokines as regulators of human hematopoietic stem cell mobilization. J Bone Miner Metab. 2018;36(4):399-409.

9. Ho M, Dasari S, Visram A, et al. An atlas of the bone marrow bone proteome in patients with dysproteinemias. Blood Cancer J. 2023;13(1):63.

10. Breczko W, Lemancewicz D, Dzięcioł J, Kłoczko J, Bołkun Ł. High immunoproteasome concentration in the plasma of patients with newly diagnosed multiple myeloma treated with bortezomib is predictive of longer OS. Adv Med Sci. 2021;66(1):21-27.

11. Fu W, Song Y, Zhao R, Zhao J, Yue Y, Zhang R. Proteomics analysis of serum and urine identifies VCP and CTSA as potential biomarkers associated with multiple myeloma. Clin Chim Acta. 2024;552:117701.

12. Xu C, Gao M, Zhang J, Fu Y. IL5RA as an immunogenic cell death-related predictor in progression and therapeutic response of multiple myeloma. Sci Rep. 2023;13(1):8528.

13. Gupta VA, Matulis SM, Conage-Pough JE, et al. Bone marrow microenvironment-derived signals induce Mcl-1 dependence in multiple myeloma. Blood. 2017;129(14):1969-1979.

14. Mielnik M, Szudy-Szczyrek A, Homa-Mlak I, et al. The clinical relevance of selected cytokines in newly diagnosed multiple myeloma patients. Biomedicines. 2023;11(11):3012.

15. Liu Y, Jie X, Nian L, et al. A combination of pre-infusion serum ferritin, CRP and IL-6 predicts outcome in relapsed/refractory multiple myeloma patients treated with CAR-T cells. Front Immunol. 2023;14:1169071.

16. Dowling P, Hayes C, Ting KR, et al. Identification of proteins found to be significantly altered when comparing the serum proteome from multiple myeloma patients with varying degrees of bone disease. BMC Genomics. 2014;15(1):904.

17. Klein B, Zhang XG, Jourdan M, et al. Paracrine rather than autocrine regulation of myeloma-cell growth and differentiation by interleukin-6. Blood. 1989;73(2):517-526.

18. Abe M, Hiura K, Wilde J, et al. Osteoclasts enhance myeloma cell growth and survival via cell-cell contact: a vicious cycle between bone destruction and myeloma expansion. Blood. 2004;104(8):2484-2491.

19. Noonan K, Marchionni L, Anderson J, Pardoll D, Roodman GD, Borrello I. A novel role of IL-17-producing lymphocytes in mediating lytic bone disease in multiple myeloma. Blood. 2010;116(18):3554-3563.

20. Dunphy K, O'Mahoney K, Dowling P, O'Gorman P, Bazou D. Clinical proteomics of biofluids in haematological malignancies. Int J Mol Sci 2021;22(15):8021.

21. Bhawal R, Oberg AL, Zhang S, Kohli M. Challenges and opportunities in clinical applications of blood-based proteomics in cancer. Cancers (Basel). 2020;12(9):2428.

22. Nikolaou PE, Mylonas N, Makridakis M, et al. Cardioprotection by selective SGLT-2 inhibitors in a non-diabetic mouse model of myocardial ischemia/reperfusion injury: a class or a drug effect? Basic Res Cardiol. 2022;117(1):27.

23. Efentakis P, Lamprou S, Makridakis M, et al. Mineralocorticoid receptor pathway is a key mediator of carfilzomib-induced nephrotoxicity: preventive role of eplerenone. Hemasphere. 2022;6(11):e791.

24. Nikolaou PE, Efentakis P, Abu Qourah F, et al. Chronic empagliflozin treatment reduces myocardial infarct size in nondiabetic mice through STAT-3-mediated protection on microvascular endothelial cells and reduction of oxidative stress. Antioxid Redox Signal. 2021;34(7):551-571.

25. Mokou M, Klein J, Makridakis M, et al. Proteomics based identification of KDM5 histone demethylases associated with cardiovascular disease. EBioMedicine 2019;41:91-104.

26. Lygirou V, Latosinska A, Makridakis M, et al. Plasma proteomic analysis reveals altered protein abundances in cardiovascular disease. J Transl Med. 2018;16(1):104.

27. Stroggilos R, Mokou M, Latosinska A, et al. Proteome-based classification of nonmuscle invasive bladder cancer. Europena Urology Supplements. 2019;18(11):e3407.

28. Margelos T, Makridakis M, Gonidaki C, et al. Simple, fast, and reliable analysis of label-free proteomics data with the proteomics eye (ProtE). PROTEOMICS – Clin Appl. 2026;20(1):e70037.

29. Wang J, Vasaikar S, Shi Z, Greer M, Zhang B. WebGestalt 2017: a more comprehensive, powerful, flexible and interactive gene set enrichment analysis toolkit. Nucleic Acids Res. 2017;45(W1):W130-W137.

30. Liao Y, Wang J, Jaehnig EJ, Shi Z, Zhang B. WebGestalt 2019: gene set analysis toolkit with revamped UIs and APIs. Nucleic Acids Res. 2019;47(W1):W199-W205.

31. Chakroborty D, Emani MR, Klén R, et al. L1TD1 - a prognostic marker for colon cancer. BMC Cancer. 2019;19(1):727.

32. Rangasamy D, Lenka N, Ohms S, Dahlstrom JE, Blackburn AC, Board PG. Activation of LINE-1 retrotransposon increases the risk of epithelial-mesenchymal transition and metastasis in epithelial cancer. Curr Mol Med. 2015;15(7):588-597.

33. Terpos E, Ntanasis-Stathopoulos I, Christoulas D, et al. Semaphorin 4D correlates with increased bone resorption, hypercalcemia, and disease stage in newly diagnosed patients with multiple myeloma. Blood Cancer J. 2018;8(5):42.

34. Terpos E, Christoulas D, Kastritis E, et al. High levels of periostin correlate with increased fracture rate, diffuse MRI pattern, abnormal bone remodeling and advanced disease stage in patients with newly diagnosed symptomatic multiple myeloma. Blood Cancer J. 2016;6(10):e482.

35. Terpos E, Kastritis E, Christoulas D, et al. Circulating activin-A is elevated in patients with advanced multiple myeloma and correlates with extensive bone involvement and inferior survival; no alterations post-lenalidomide and dexamethasone therapy. Ann Oncol. 2012;23(10):2681-2686.

36. Neufeld G, Sabag AD, Rabinovicz N, Kessler O. Semaphorins in angiogenesis and tumor progression. Cold Spring Harb Perspect Med. 2012;2(1):a006718.

37. Yazdani U, Terman JR. The semaphorins. Genome Biol .2006;7(3):211.

38. Terpos E, Ntanasis-Stathopoulos I, Christoulas D, et al. Semaphorin 4D correlates with increased bone resorption, hypercalcemia, and disease stage in newly diagnosed patients with multiple myeloma. Blood Cancer J. 2018;8(5):42.

39. Worzfeld T, Offermanns S. Semaphorins and plexins as therapeutic targets. Nat Rev Drug Discov. 2014;13(8):603-621.

40. Suvannasankha A, Crean CD, Tompkins DR, et al. Regulation of osteoblast function in myeloma bone disease by semaphorin 4D. Blood. 2016;128(22):4439.

41. Lontos K, Adamik J, Zhang P, et al. Semaphorin 4D to suppress bone formation in multiple myeloma. J Clin Oncol. 2017;35(15_suppl):8039.

42. Nobari ST, Rasmi Y, Khadem Ansari MH. Serum levels of interleukin-1β and disease progression in multiple myeloma patients: a case and control study. Asian Pac J Cancer Prev. 2022;23(9):2937-2942.

43. Mazurek M, Szudy-Szczyrek A, Homa-Mlak I, Hus M, Małecka-Massalska T, Mlak R. IL1B polymorphism (rs1143634) and IL-1β plasma concentration as predictors of nutritional disorders and prognostic factors in multiple myeloma patients. Cancers (Basel). 2024;16(7):1263.

44. Zhu Z, Luo Y, Yu J, et al. Sema4D is required in both the adaptive and innate immune responses of contact hypersensitivity. Mol Immunol. 2016;78:98-104.

45. Ho BHT, Spicer BA, Dunstone MA. Action of the terminal complement pathway on cell membranes. J Membr Biol. 2025;258(4):269-304.

46. Mödinger Y, Löffler B, Huber-Lang M, Ignatius A. Complement involvement in bone homeostasis and bone disorders. Semin Immunol. 2018;37:53-65.

47. Risitano AM, Frieri C, Urciuoli E, Marano L. The complement alternative pathway in paroxysmal nocturnal hemoglobinuria: From a pathogenic mechanism to a therapeutic target. Immunol Ver. 2023;313(1):262-278.

48. Terpos E, Zamagni E, Lentzsch S, et al. Treatment of multiple myeloma-related bone disease: recommendations from the Bone Working Group of the International Myeloma Working Group. Lancet Oncol. 2021;22(3):e119-e130.

49. Yong K, Delforge M, Driessen C, et al. Multiple myeloma: patient outcomes in real-world practice. Br J Haematol. 2016;175(2):252-264.

50. Wang SS, Abdou AM, Morton LM, et al. Human leukocyte antigen class I and II alleles in non-Hodgkin lymphoma etiology. Blood. 2010;115(23):4820-4823.

51. Alcoceba M, Sebastián E, Marín L, et al. HLA specificities are related to development and prognosis of diffuse large B-cell lymphoma. Blood. 2013;122(8):1448-1454.

52. Beksac M, Maiers M, Gragert L, et al. HLA specificities and predisposition to the development of multiple myeloma (MM). Blood. 2008;112(11):1688.

Figure legends

Figure 1. ELISA analysis of SEMA4D (A), periostin (B) and activin-A (C) in SMM/MGUS and newly diagnosed multiple myeloma (NDMM) patients. Graphs present data from SMM/MGUS patients who did not progress to MM (non-progressors; n=25; grey color), SMM/MGUS patients who progressed to NDMM with (n=15) and without MBD (n=6) and NDMM patients with (n =31) and without (n = 19) MBD. Patients who progressed from MGUS/SMM to MM (n = 21) are marked in red or light red. Individual and mean values ± SD are shown. Statistical analysis was performed using one-way ANOVA followed by Tukey's post hoc test. *p<0.05, **p<0.01, ***p<0.001.

Figure 2. Univariate Kaplan–Meier survival analysis according to SEMA4D levels in newly diagnosed multiple myeloma (NDMM) patients. (A) Kaplan–Meier curve for progression-free survival (PFS) stratified by SEMA4D levels (high vs low). (B) Kaplan–Meier curve for time to progression (TTP) stratified by SEMA4D levels (high vs low). Patients were dichotomized based on an optimal cutoff value which was defined via maximal ranked statistics. Survival differences between groups were evaluated using the log-rank test.

Figure 3: Prognostic significance of IL-1β and OPG in newly diagnosed multiple myeloma (NDMM) patients. (A) Kaplan–Meier curve for progression-free survival (PFS) stratified by IL-1β levels (high vs low) using an optimal cutoff determined by maximally selected rank statistics. Elevated IL-1β levels were associated with inferior PFS. (B) Kaplan–Meier curve for overall survival (OS) stratified by osteoprotegerin (OPG) levels (high vs low) using the optimal cutoff determined by maximally selected rank statistics. Higher OPG levels were associated with reduced OS; however,

interpretation is limited by the small number of events. Survival differences were assessed using the log-rank test.

Figure 4: Barplots of circulating markers of proteome profiling stratified by the presence of myeloma bone disease (MBD) in NDMM patients. Mann-Whitney test was applied, and p values are depicted prior to FDR adjustments. P values are shown on the graphs.

Figure 5: Identification and pathway characterization of a common outcome-related protein signature. (A) Venn diagram illustrating proteins commonly associated with all three major outcome parameters based on multivariate analysis, identifying a shared signature of 13 proteins (i.e., IGKV2-30, CFP, MASP1, F9, CLEC3B, ATRN, FGB, BCHE, ITIH4, C5, CPN1, LRG1, and PLG). (B) Pathway enrichment analysis of the common protein signature performed using WebGestalt with Reactome pathway annotations, demonstrating predominant clustering in complement activation, platelet function, and hemostatic pathways, including initial triggering and regulation of the complement cascade and activation of C3 and C5.

Figure 6: Circulating complement C5 determines disease progression. (A) Kaplan–Meier curve for progression-free survival (PFS) stratified by C5 levels (high vs low) using the optimal cutoff (281.44). Patients with elevated C5 levels exhibited significantly shorter PFS. (B) Kaplan–Meier curve for time to progression (TTP) stratified by C5 levels (high vs low) using the optimal cutoff (281.44). High C5 levels were associated with inferior TTP. Patients were dichotomized according to the optimal cutoff value derived from maximal rank statistics. Survival differences were assessed using the log-rank test.

Figure 7: Overall survival does not significantly differ between NDMM patients with and without myeloma bone disease (MBD). Kaplan–Meier curve for overall survival in patients with NDMM, stratified according to the presence (red curve) or absence (blue curve) of MBD.

Figure 8: Progression free survival and time-to-progression do not significantly differ between NDMM patients with and without myeloma bone disease (MBD). A) Kaplan–Meier curve for progression free survival in patients with NDMM, stratified according to the presence (red curve) or absence (blue curve) of MBD. B) Kaplan–Meier curve for time to progression in patients with NDMM, stratified according to the presence (red curve) or absence (blue curve) of MBD.

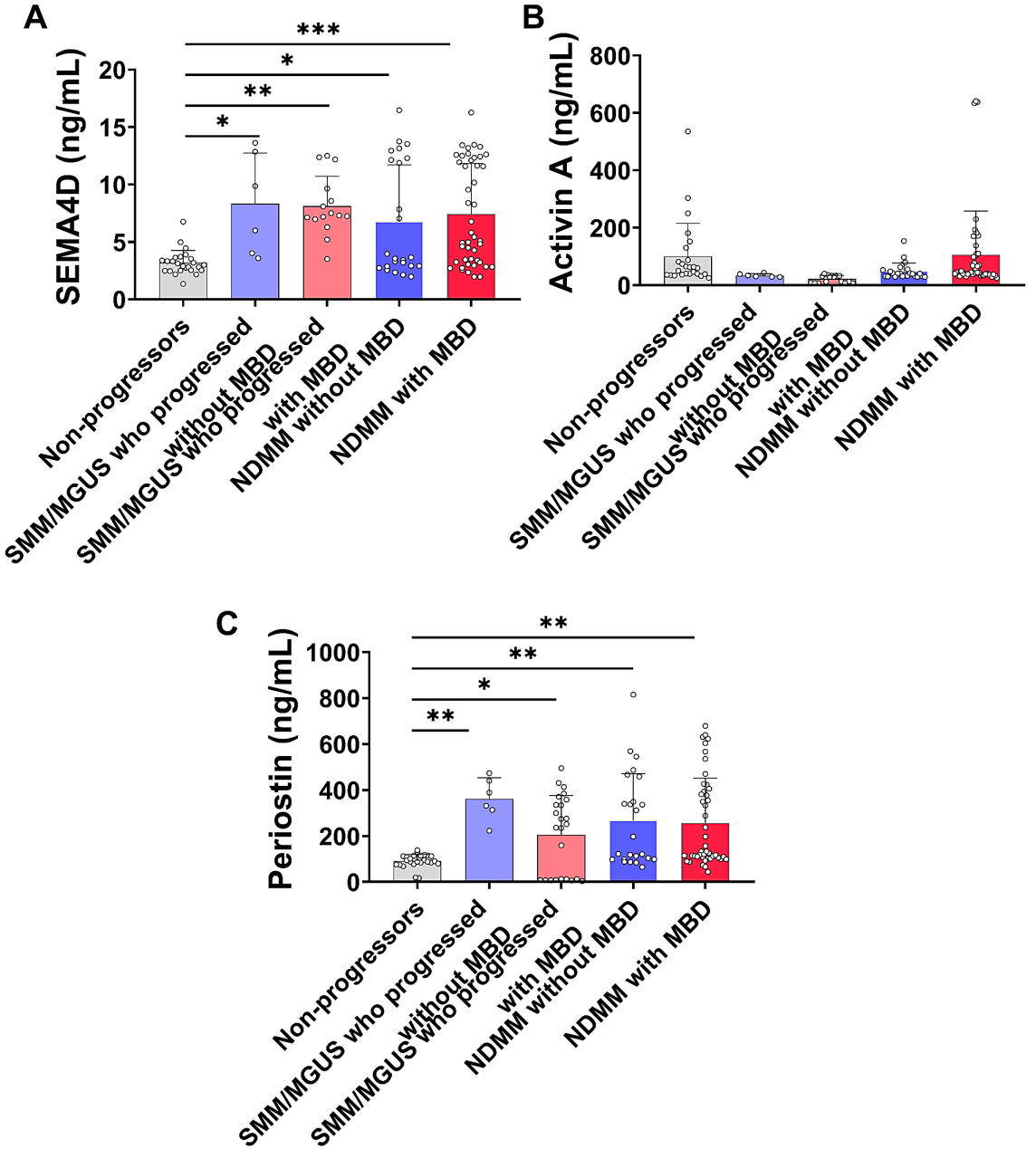
A
SEMA4D (ng/mL)
0
5
10
15
20
*
**
*
***
Non-progressors
SMM/MGUS who progressed
SMM/MGUS who progressed
NDMM without MBD
NDMM with MBD
without MBD
with MBD
B
Activin A (ng/mL)
0
200
400
600
800
Non-progressors
SMM/MGUS who progressed
SMM/MGUS who progressed
NDMM without MBD
NDMM with MBD
without MBD
with MBD
C
Periostin (ng/mL)
0
200
400
600
800
1000
**
*
**
**
Non-progressors
SMM/MGUS who progressed
SMM/MGUS who progressed
NDMM without MBD
NDMM with MBD
without MBD
with MBD

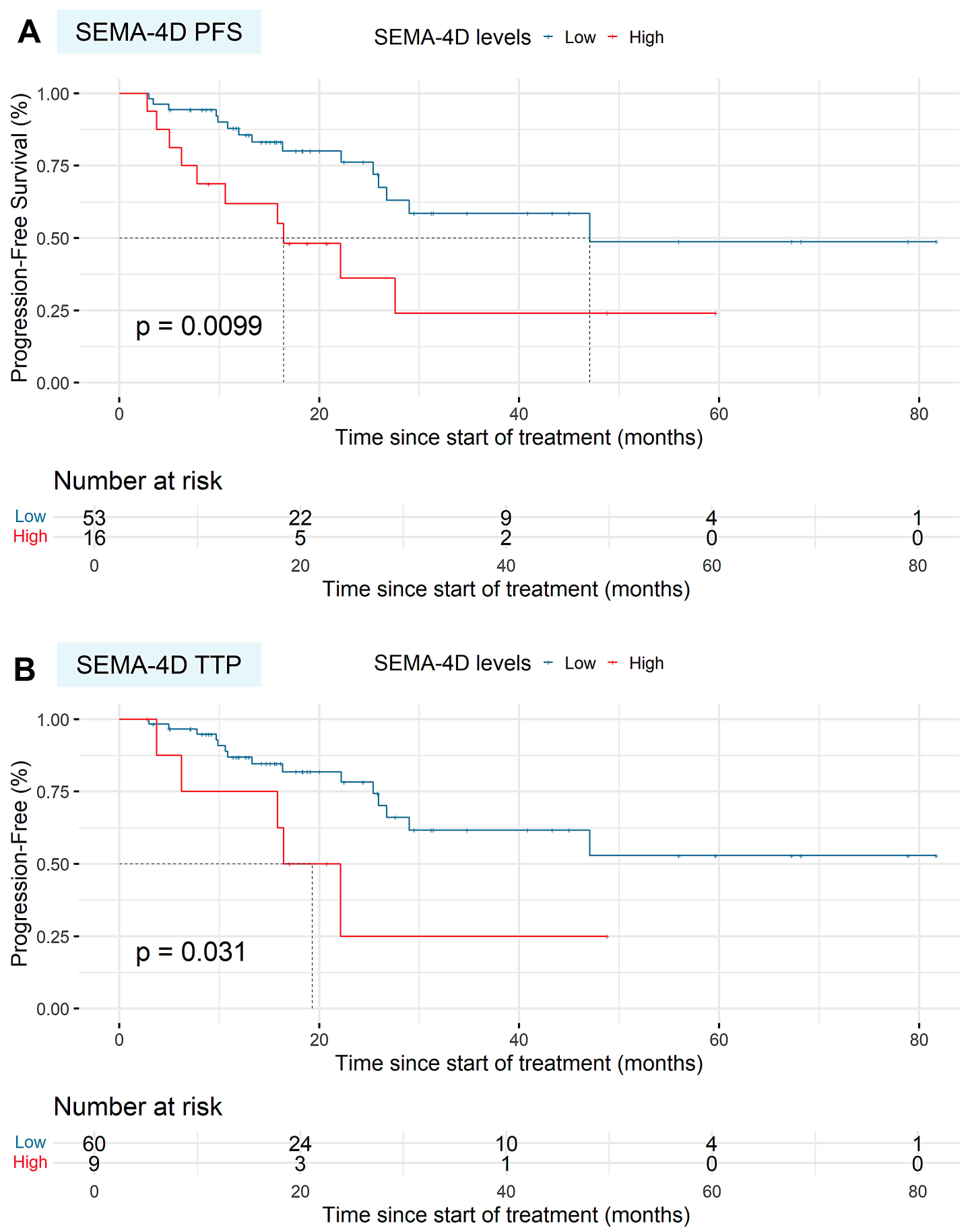
A
SEMA-4D PFS
SEMA-4D levels
Low
High
Progression-Free Survival (%)
1.00
0.75
0.50
0.25
0.00
p = 0.0099
0
20
40
60
80
Time since start of treatment (months)
Number at risk
Low 53 22 9 4 1
High 16 5 2 0 0
0
20
40
60
80
Time since start of treatment (months)
B
SEMA-4D TTP
SEMA-4D levels
Low
High
Progression-Free (%)
1.00
0.75
0.50
0.25
0.00
p = 0.031
0
20
40
60
80
Time since start of treatment (months)
Number at risk
Low 60 24 10 4 1
High 9 3 1 0 0
0
20
40
60
80
Time since start of treatment (months)

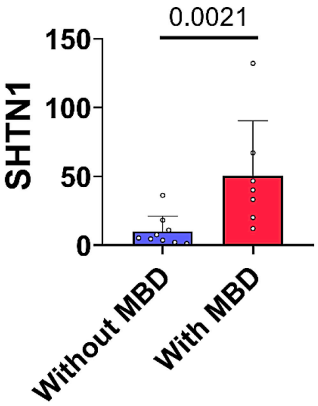
SHTN1
0.0021
150
100
50
0
Without MBD
With MBD

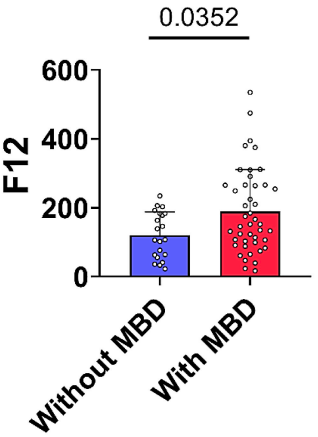
F12
0.0352
600
400
200
0
Without MBD
With MBD

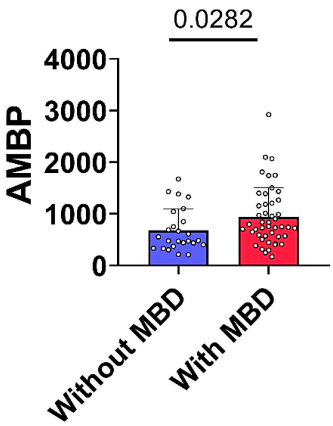
AMBP
0.0282
4000
3000
2000
1000
0
Without MBD
With MBD

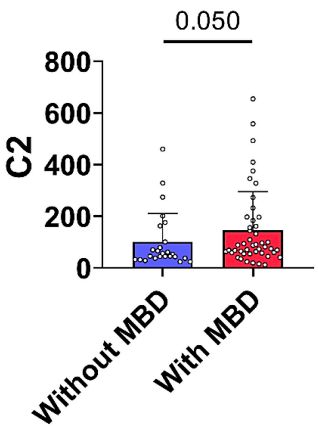
C2
0.050
800
600
400
200
0
Without MBD
With MBD

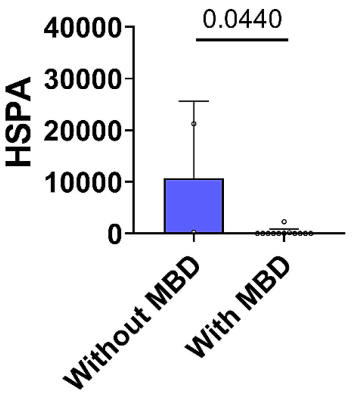
HSPA
0.0440
40000
30000
20000
10000
0
Without MBD
With MBD

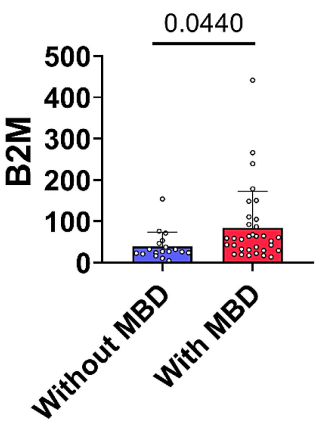
B2M
0.0440
500
400
300
200
100
0
Without MBD
With MBD

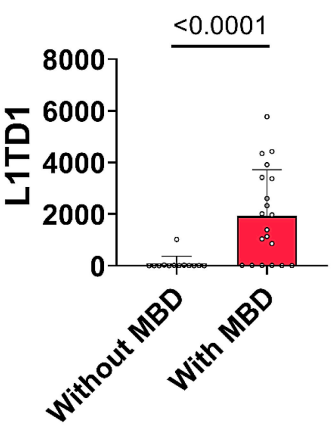
L1TD1
<0.0001
8000
6000
4000
2000
0
Without MBD
With MBD

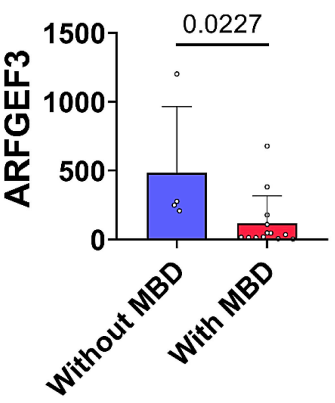
ARFGEF3
0.0227
1500
1000
500
0
Without MBD
With MBD

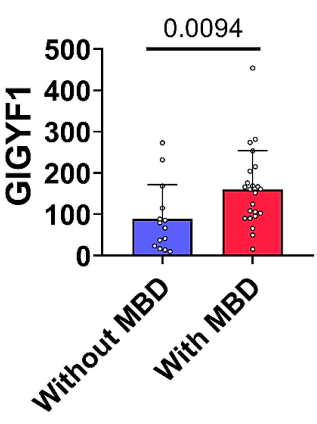
GIGYF1
0.0094
500
400
300
200
100
0
Without MBD
With MBD

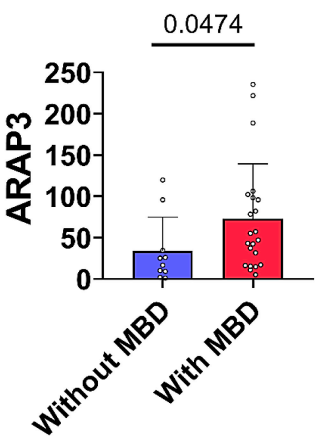
ARAP3
0.0474
250
200
150
100
50
0
Without MBD
With MBD

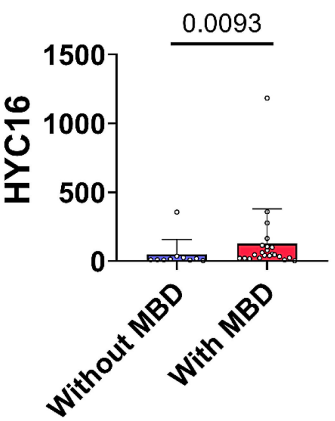
HYC16
0.0093
1500
1000
500
0
Without MBD
With MBD

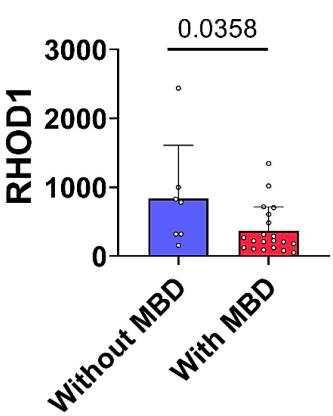
RHOD1
0.0358
3000
2000
1000
0
Without MBD
With MBD

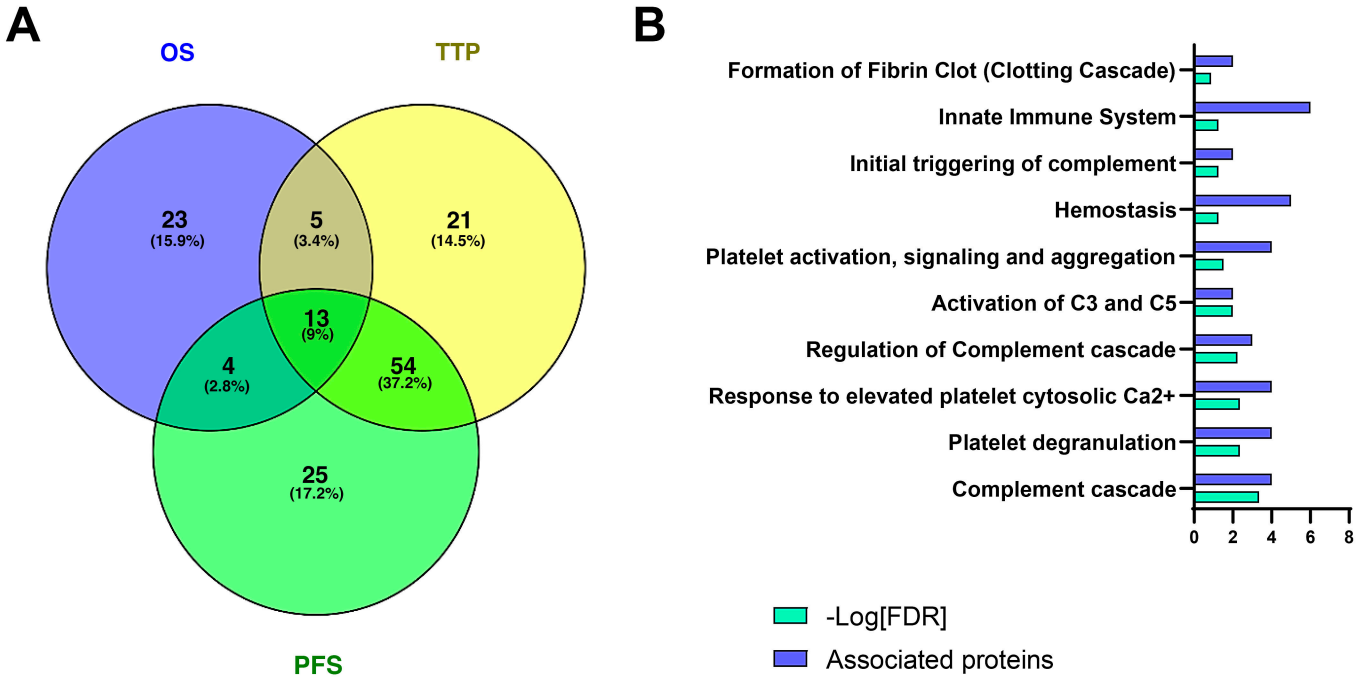
A
OS
TTP
PFS
23
(15.9%)
5
(3.4%)
21
(14.5%)
13
(9%)
4
(2.8%)
54
(37.2%)
25
(17.2%)
B
Formation of Fibrin Clot (Clotting Cascade)
Innate Immune System
Initial triggering of complement
Hemostasis
Platelet activation, signaling and aggregation
Activation of C3 and C5
Regulation of Complement cascade
Response to elevated platelet cytosolic Ca2+
Platelet degranulation
Complement cascade
0
2
4
6
8
-Log[FDR]
Associated proteins

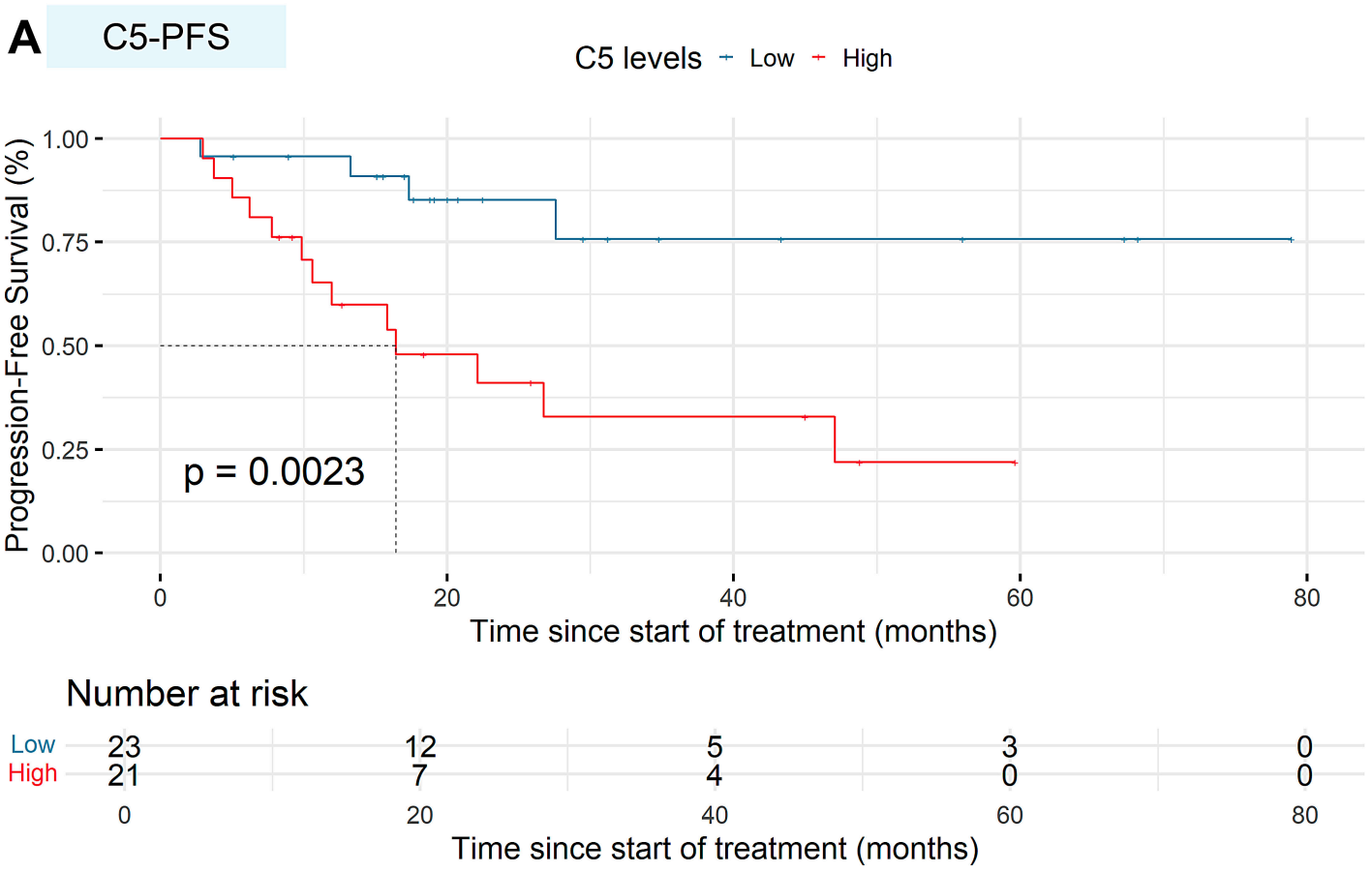
A
C5-PFS
C5 levels
Low
High
Progression-Free Survival (%)
1.00
0.75
0.50
0.25
0.00
p = 0.0023
0
20
40
60
80
Time since start of treatment (months)
Number at risk
Low
High
23
12
5
3
0
21
7
4
0
0
0
20
40
60
80
Time since start of treatment (months)

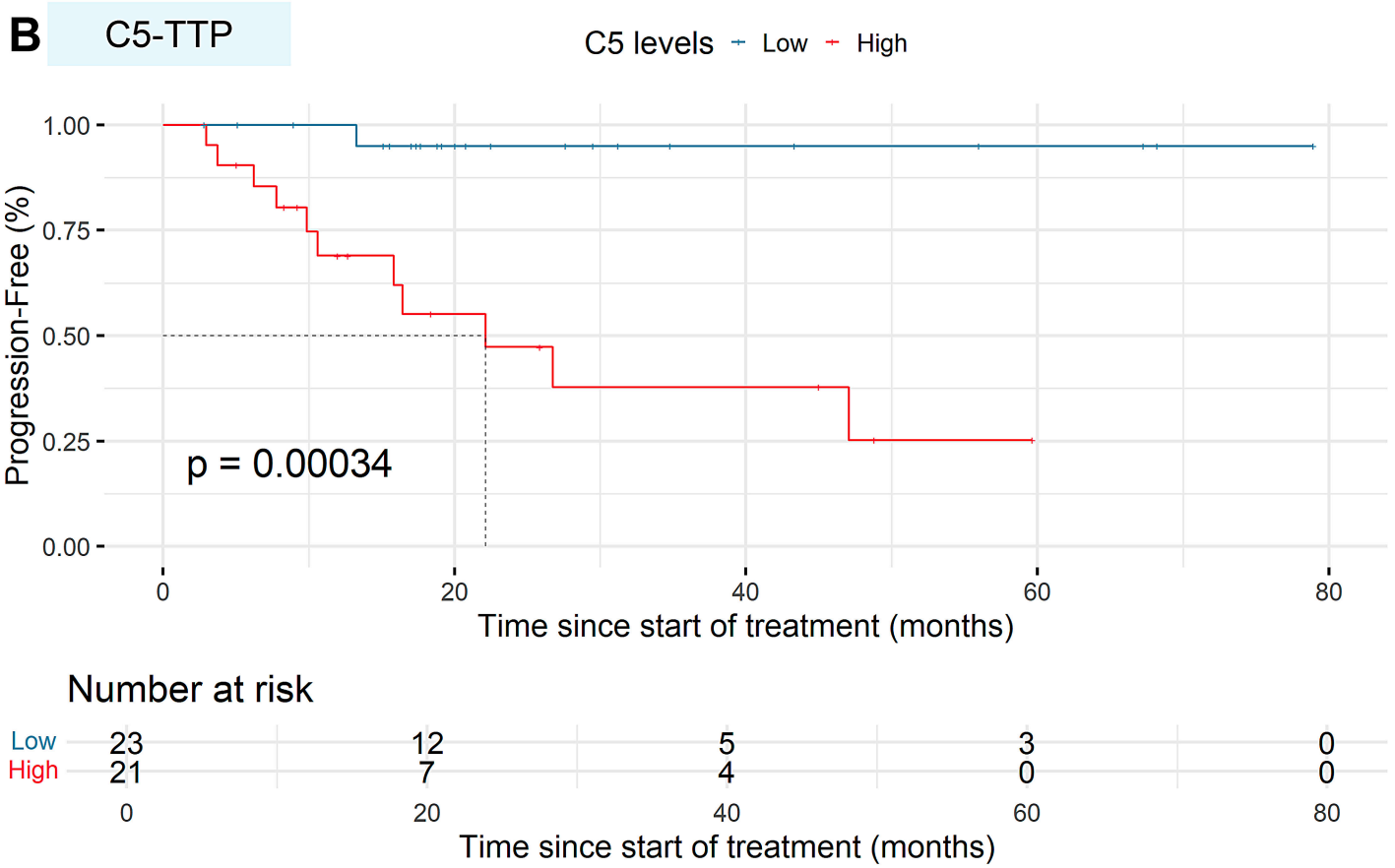
B
C5-TTP
C5 levels
Low
High
Progression-Free (%)
1.00
0.75
0.50
0.25
0.00
p = 0.00034
0
20
40
60
80
Time since start of treatment (months)
Number at risk
Low
High
23
12
5
3
0
21
7
4
0
0
0
20
40
60
80
Time since start of treatment (months)

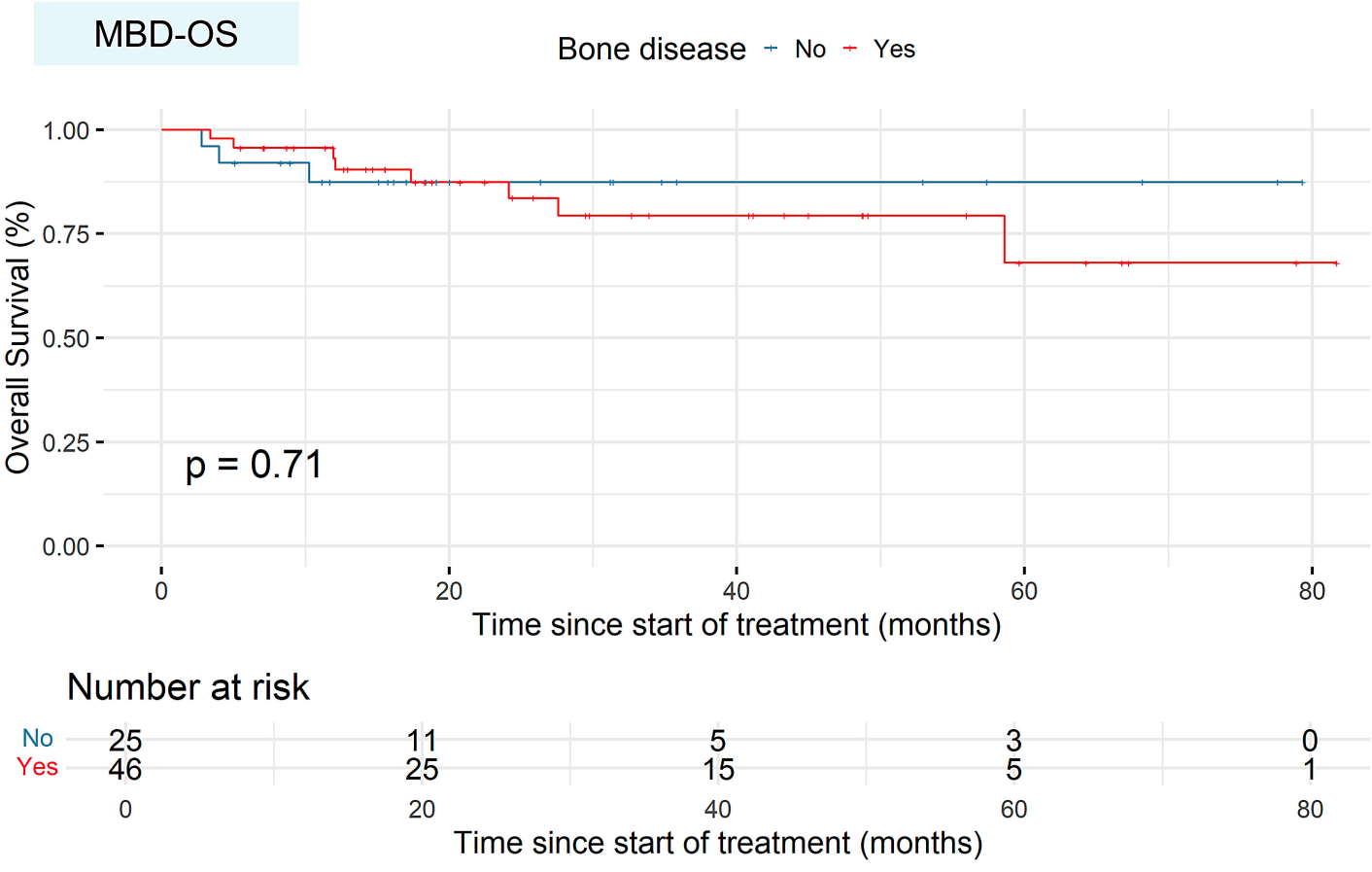
MBD-OS
Bone disease
No
Yes
1.00
0.75
0.50
0.25
0.00
Overall Survival (%)
p = 0.71
0
20
40
60
80
Time since start of treatment (months)
Number at risk
No
Yes
25
46
11
25
5
15
3
5
0
1
0
20
40
60
80
Time since start of treatment (months)

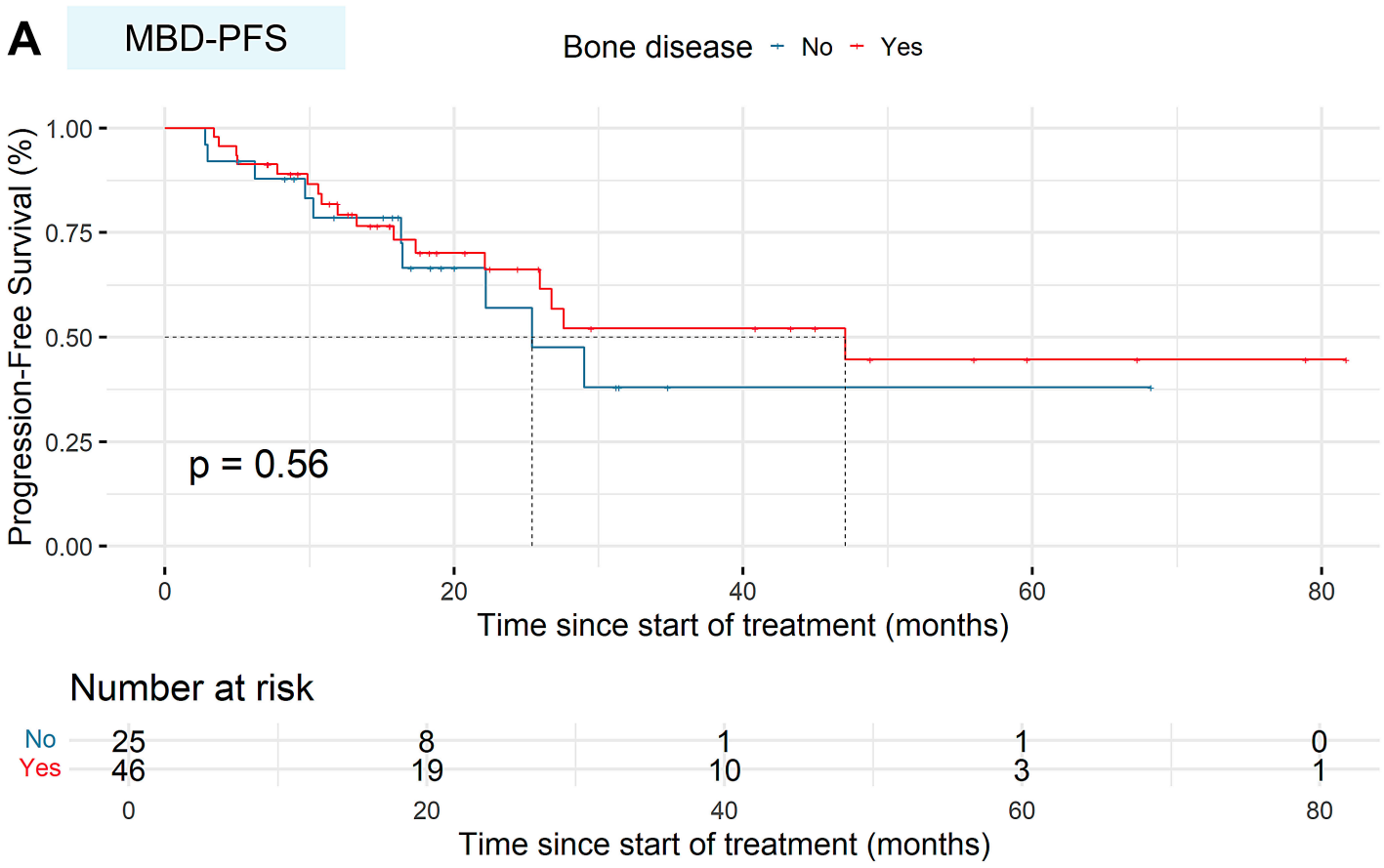
A
MBD-PFS
Bone disease
No
Yes
Progression-Free Survival (%)
1.00
0.75
0.50
0.25
0.00
p = 0.56
0
20
40
60
80
Time since start of treatment (months)
Number at risk
No
Yes
25
8
1
1
0
46
19
10
3
1
0
20
40
60
80
Time since start of treatment (months)

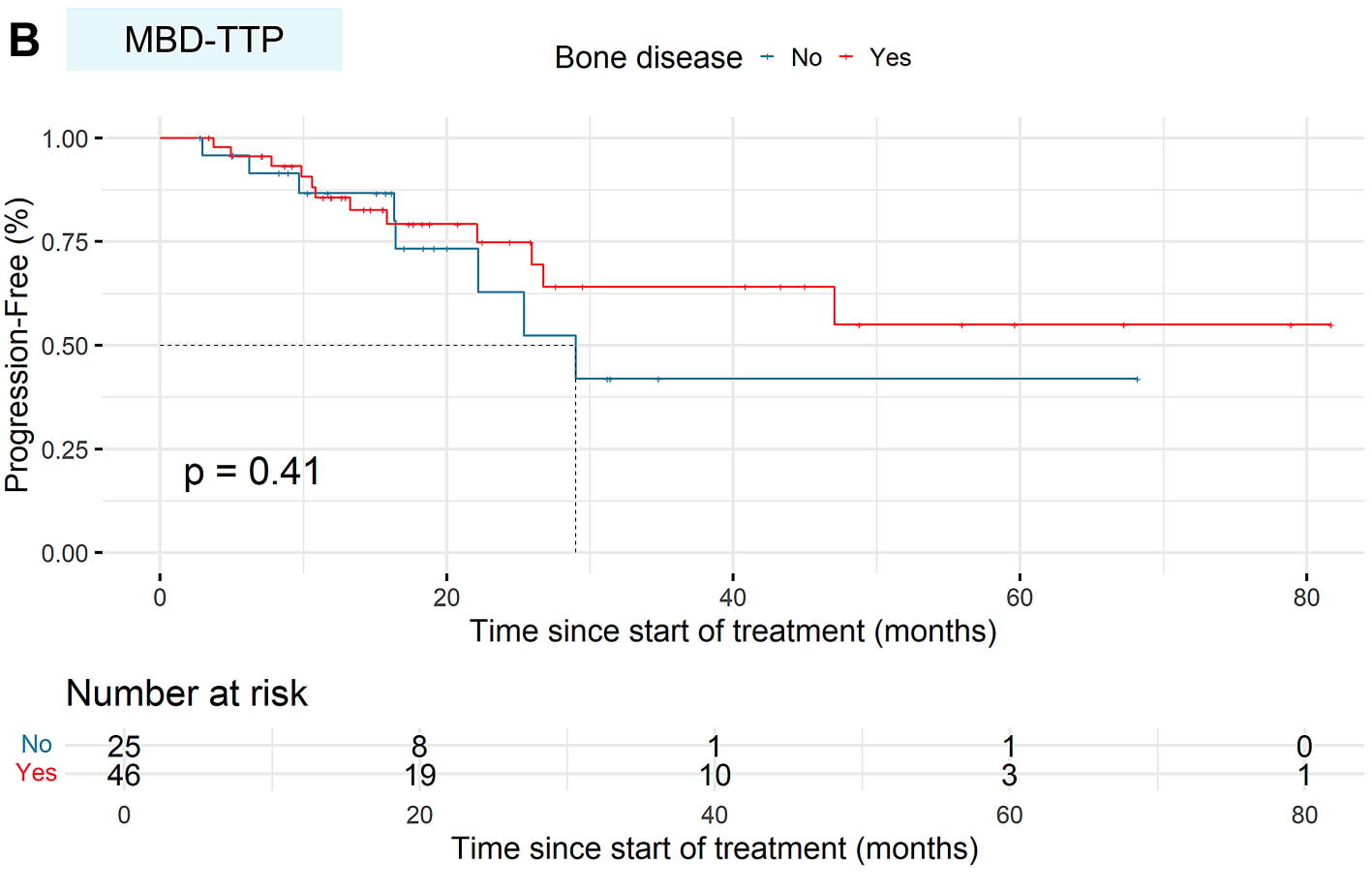
B
MBD-TTP
Bone disease
No
Yes
Progression-Free (%)
1.00
0.75
0.50
0.25
0.00
p = 0.41
0
20
40
60
80
Time since start of treatment (months)
Number at risk
No
Yes
25
8
1
1
0
46
19
10
3
1
0
20
40
60
80
Time since start of treatment (months)

Independent prognostic value of Semaphorin-4D, interleukin-1β and complement activation in newly diagnosed multiple myeloma patients

Ioannis Ntanasis-Stathopoulos*[1], Panagiota-Efstathia Nikolaou*[1,2], Charalampos Filippatos[1], Marios Miliotis[3], Ioannis V Kostopoulos[4], Panagiotis Bakouros[4], Manousos Makridakis[5], Christine-Ivy Liacos[1], Konstantinos Nikolopoulos[2], Stamatia Laidou[6], Anastasia Chatzidimitriou[6,7], Maria Frantzi[8], Efstathios Kastritis[1], Despina Fotiou[9], Maria Gavriatopoulou[1], Antonia Vlahou[5], Artemis G Hatzigeorgiou[3], Ourania Tsitsilonis[4], Meletios Athanasios Dimopoulos[1,10], Evangelos Terpos[1#].

(1) Department of Clinical Therapeutics, Alexandra Hospital, School of Medicine, National and Kapodistrian University of Athens, Athens, Greece

(2) Laboratory of Pharmacology, Faculty of Pharmacy, National and Kapodistrian University of Athens, Athens, Greece

(3) DIANA-Lab, Department of Computer Science and Biomedical Informatics, University of Thessaly, Lamia, Greece

(4) Section of Animal and Human Physiology, Department of Biology, National and Kapodistrian University of Athens, Athens, Greece

(5) Laboratory of Biotechnology, Academy of Athens Biomedical Research Foundation, Athens, Greece

(6) Institute of Applied Biosciences, Centre for Research and Technology Hellas, Thessaloniki, Greece.

(7) Department of Molecular Medicine and Surgery, Karolinska Institutet, Stockholm, Sweden.

(8) Department of Biomarker Research, Mosaiques diagnostics GmbH, 30659 Hannover, Germany

(9) Department and Laboratory of Pathophysiology, Medical School, National and Kapodistrian University of Athens, Athens, Greece

(10) Department of Medicine, Korea University, Seoul, South Korea

#Address of correspondence: Professor Evangelos Terpos, Department of Clinical Therapeutics, Alexandra Hospital, School of Medicine, National and Kapodistrian University of Athens, 80 Vas. Sophias Ave, 11528 Athens, Greece; email: eterpos@med.uoa.gr; tel: +302132162846

*The authors have equally contributed to this work

Supplementary methods

Supplementary materials

All reagents were purchased from Sigma Aldrich (St. Louis, MI) or Macherey-Nagel (Duren, DE), while ELISA kits were purchased from LSBio via ELTA90MGR.

Plasma collection

Peripheral blood was collected in EDTA-anticoagulated tubes and centrifuged at 3,000 × g for 10 min at room temperature. The supernatant plasma was carefully collected, transferred to clean tubes, and stored at −80°C until further analysis. Freeze–thaw cycles were avoided.

Quantification of circulating biomarkers by ELISA

Plasma concentrations of SEMA4D, activin-A, and periostin were quantified using commercially available sandwich ELISA kits (Human SEMA4D ELISA Kit, Cat. No. LS-F22167-1; Human Activin A ELISA Kit, Cat. No. LS-F54506-1; Periostin ELISA Sandwich Kit, Cat. No. LS-F3645; all from LSBio, Shirley, MA), according to the manufacturers' instructions.

Briefly, plasma samples were thawed on ice and analyzed in duplicate. Optical density was measured using a Tecan Infinite® M200 PRO microplate reader (Tecan Group Ltd., Männedorf, Switzerland) at the recommended wavelength, and concentrations were calculated from standard curves generated using recombinant standards provided with each kit. Intra- and inter-assay variability were within the ranges specified by the manufacturers.

Multiplex analysis of bone metabolism–related proteins

To quantify additional circulating markers related to bone metabolism and inflammation using the LEGENDplex™ Human Bone Metabolism Panel (13-plex; BioLegend, San Diego, CA, USA), a multiplex bead-based immunoassay. The panel allows the simultaneous quantification of 13 proteins, including cytokines and bone-related mediators, in small plasma volumes. Standard curves were constructed for osteoprotegerin (OPG), osteopontin (OPN), platelet-derived growth factor-BB (PDGF-BB), alkaline phosphatase (ALPL), tartrate-resistant acid phosphatase 5 (ACP5), leptin, receptor activator of nuclear factor-κB ligand (RANKL/TRANCE), tumor necrosis factor-α (TNF-α), interleukin-6 (IL-6), parathyroid hormone (PTH), interleukin-1β (IL-1β), bone morphogenetic protein-2 (BMP-2), and Dickkopf-1 (DKK-1). Data acquisition was performed using a BD FACSCanto II cytometer (BD Biosciences, San Jose, CA) and analyte concentrations were determined based on standard curves generated from serial dilutions of provided standards, according to the manufacturer's instructions, mean fluorescence intensity (MFI) was plotted against known analyte concentrations and curves were generated using a five-parameter logistic (5-PL) regression model. Data analysis was conducted using the LEGENDplex™ Data Analysis Software, with concentration values expressed in pg/mL. Quality control procedures, including bead count thresholds and standard curve acceptance criteria, were applied according to the manufacturer's recommendations.

Proteomics

Sample processing for proteomic analysis

Plasma samples were collected and processed for proteomic analysis. The filter aided sample preparation (FASP) was performed as we have previously reported.[1–3] Plasma

volume corresponding to a total protein content of 200 µg for each sample was mixed with 200 µL of urea buffer (8 M Urea in 0.1 M Tris–HCl pH 8.5; UA buffer), reduced with 10mM DTE for 20 min RT and placed in Amicon filter units (0.5 ml, 30 kDa MW cutoff). The units were centrifuged at 14,000 × *g* for 15 min twice and the flow-through was discarded. Subsequently, 100 µL of 0.05 M Iodoacetamide in UA buffer were added and incubated for 20 min in the dark at room temperature (protein alkylation). The filter units were centrifuged at 14,000 × *g* for 10 min, the flow through was discarded, washed with equivalent volume of UA buffer and centrifuged again. Afterwards, 100 µL of ammonium bicarbonate buffer (50 mM NH_4HCO_3 in ultrapure water, pH 8.5) were added to the filter unit and centrifuged at 14,000 × *g* for 10 min twice. Finally, the samples were trypsinized in a humidity container overnight at room temperature in the dark using a solution of 50 mM NH_4HCO_3 pH 8.5, and trypsin to protein ratio 1:100 (w/w). Elution of the peptides was performed after centrifugation of the filter units at 14,000 × *g* for 10 min. Centrifugation was repeated after a second addition of 40 µL 50 mM NH_4HCO_3 pH 8.5 into the filter units. Eluted peptides were lyophilized and stored at − 80 °C until analysis.

All LC-MS/MS experiments were conducted using the Dionex Ultimate 3000 UHPLC system coupled with the high-resolution nano-ESI Q-Exactive Plus - Orbitrap mass spectrometer (Thermo Scientific, Waltham, MA). Each sample was reconstituted in 100 µL of mobile phase A (98% water, 2% acetonitrile and 0.1% formic acid), and then diluted to 0.2 µg/µL. A 5 µL volume, equivalent to 1 µg of protein, was injected and loaded onto an PepMap Neo C18 5 µm trapping column (300 µm × 5 mm, 1500 bar) using the micro-injection PickUp method, with the loading pump operating at a flow rate of 30 µL/min. For peptide separation, the Acclaim PepMap 100 column (75 µm ×

50 cm, nanoViper, C18, 3 µm, 100 Å) was used, connected to a PicoTip emitter, with a multi-step gradient elution. The mobile phase A consisted of 2% acetonitrile with 0.1% formic acid, and mobile phase B consisted of 80% acetonitrile, 0.1% formic acid. Peptides were eluted under a 250-min gradient from 2% (B) to 95% (B). The flow rate and column temperature were set to 300 nL/min and 40°C, respectively. The transition to the gas phase of the separated peptides was achieved by positive ion spray, applying a voltage of 1.8 kV. For each MS scan, the 20 most abundant multiply charged precursor ions between the m/z ratio of 380 and 1200, were selected for FT mass analysis at a resolution of 70,000 and subjected to higher-energy collision dissociation (HCD). The combined mass spectrum was recorded with FT analysis at a resolution of 17,500. The normalized collision energy was set at 30, and previously targeted precursor ions were dynamically excluded for further isolation and activation for 15 seconds[4].

MS data processing and quantification

Raw files were analyzed with the Proteome Discoverer 1.4 software package (Thermo Finnigan, Bremen, DE), using the Sequest search engine and the Uniprot Human (Homo sapiens) reviewed database, downloaded on November 22, 2024, including 20,647 protein entries. The search was performed using carbamidomethylation of cysteine as static and oxidation of methionine as dynamic modifications. Two missed cleavage sites, a precursor mass tolerance of 10 ppm and fragment mass tolerance of 0.05 Da were allowed. False discovery rate (FDR) validation was based on q value: target FDR : 0.01[5]. Quantification was performed at the peptide level employing a clustering approach as previously described [6,7]. Label free quantification was

performed by utilizing the precursor area values of each protein as defined by the Proteome Discoverer 1.4 software package. Samples were analyzed individually and assigned to distinct groups. For a small number of peptide sequences where no peptide precursor area could be retrieved (although the peptides were identified) the missing values were replaced by zero. If a peptide was not identified in a particular sample the missing values were replaced by zero. For the quantitation-statistical analysis, only the peptides which were present in at least 25% of the samples in at least one group were further considered. The precursor area values were subjected to the following normalization method within each sample prior quantification analysis: normalized peak area = (peptide peak area/sum of peptides peak area) × 10^6. Protein expression values were calculated as the sum of all the normalized peptide areas that were assigned for a given protein. *P* value ≤0.05 was considered statistically significant. Differential protein expression analysis was performed using the ProtE R package[8]. Pathway enrichment analysis of proteins of interest was conducted using the web-based GEne SeT AnaLysis Toolkit (WebGestalt) [9,10].

Genomics

Clonal plasma cell and bulk cells sorting

Clonal plasma cells and non-clonal BM populations were sorted from a sub-cohort of n=25 NDMM patients. Cryopreserved BM mononuclear cells of these patients were stored at diagnosis in liquid nitrogen in cryovials containing 90% fetal bovine serum (FBS) and 10% dimethyl sulfoxide (DMSO). For thawing, vials were rapidly transferred from liquid nitrogen to a 37°C water bath and gently agitated until just a small ice

crystal remained (approximately 1–2 min). Thawed cells were immediately transferred into 15 mL conical tubes containing 10 mL of pre-warmed RPMI-1640 medium supplemented with 10% FBS, added dropwise to minimize osmotic shock. Cells were then centrifuged at 1500 × g for 5 min at room temperature. The supernatant was carefully aspirated, and the cell pellet was resuspended in PBS/ 1% FBS/ 2 mM EDTA. Cell viability and concentration were assessed using Trypan Blue exclusion.

Flow cytometry and cell sorting were performed on a BD FACSMelody™ (BD Biosciences). Live, single cells were gated using FSC-A/FSC-H and SSC-A parameters. To isolate clonal plasma cells from BM nucleated cells, we employed five key surface markers: CD38, CD45, CD19, CD56, and CD117. Regarding the gating strategy, we first gated on single cells using forward scatter (FSC) and side scatter (SSC) parameters. We then selected the $CD38^{+}CD45^{dim/-}$ population within the singlet gate to include all plasma cells. Subsequently, we identified clonal plasma cells by gating on the $CD19^{-}CD56^{+}$ subset. In samples where clonal plasma cells were known to express CD117, an additional gate was applied to isolate the $CD117^{+}$ population (***Supplementary figure 6***). Plasma cells and bulk were sorted into sterile tubes containing cold RPMI-1640 medium. Sorted cells were pelleted and used immediately for downstream DNA/RNA extraction.

<u>DNA isolation from sorted cells</u>

Total DNA was isolated from sorted cell samples using the NucleoSpin® TriPrep kit (Macherey-Nagel, Germany) following the manufacturer's protocol. Cells were lysed in 350 µL Buffer RP1 supplemented with 3.5 µL β-mercaptoethanol to inactivate

RNases, DNases, and proteases. After thorough vortexing, the lysate was filtered through a NucleoSpin® Filter and transferred to a fresh tube. Next, 350 µL of 70% ethanol was added to the lysate to facilitate binding of nucleic acids to the silica membrane. The entire volume was applied to a NucleoSpin® TriPrep Column and centrifuged to bind DNA and RNA to the membrane while proteins were collected in the flow-through. DNA was first purified by washing the column twice with 500 µL DNA Wash buffer, followed by a drying step. DNA was then eluted in 100 µL of DNA Elute buffer, incubated for 1 min, and centrifuged. This step yielded high-molecular-weight genomic DNA suitable for downstream applications such as PCR and restriction digestion. After DNA elution, the column was treated with an on-column DNase digestion step to eliminate residual DNA prior to RNA elution. A 95 µL reaction mixture containing reconstituted rDNase and DNase buffer was directly applied to the membrane and incubated at room temperature for 15 min. The column was then washed sequentially with 200 µL RA2 buffer, 600 µL RA3, and 250 µL RA3, with centrifugation at each step. RNA was eluted in 60 µL of RNase-free water by centrifugation, yielding high-integrity RNA suitable for reverse transcription and quantitative PCR. Both DNA and RNA eluates were handled under RNase- and DNase-free conditions and stored at –20°C for short-term or –70°C for long-term use. All procedures were conducted at room temperature unless otherwise stated.

Whole-exome sequencing and variant analysis

Whole-exome sequencing (WES) was performed in genomic DNA isolated from the sorted clonal plasma cells and from bulk BM nucleated cells (BMNCs), serving as the non-clonal comparator. Library preparation and whole exome enrichment were

performed using the Twist Library Preparation EF Kit and the Twist Target Enrichment Standard Hybridization v2 Protocol (Twist Bioscience, USA) following the manufacturer's instructions. Briefly, 50 ng genomic DNA was enzymatically fragmented, end-repaired, A-tailed and ligated to sequencing adapters containing unique dual indices (Twist UDI Primers). Adapter-ligated fragments were amplified by limited-cycle PCR and were purified using magnetic beads. Library quality and fragment size distribution were assessed using the Agilent Fragment Analyzer (Agilent, Santa Clara, CA, USA), targeting an average library size of approximately 300 bp prior to hybridization. Hybridization-based capture of exonic regions was performed using biotinylated probes (Twist Comprehensive Exome Panel) specific to the human exome, and probe-library complexes were retrieved using streptavidin magnetic beads. The quality and size distribution of final libraries were again confirmed on the Agilent Fragment Analyzer (Agilent, Santa Clara, CA, USA). Libraries were quantified using the KAPA Library Quantification Kit for Illumina® Platforms (Roche, Basel, Switzerland). Sequencing was performed on the Illumina NextSeq 2000 platform (Illumina, San Diego, CA, USA) to generate 150 bp paired-end reads, achieving a mean coverage depth of 90X. Sequencing reads underwent quality control with FastQC, to assess base quality, GC content and adapter contamination. Reads were aligned to human genome assembly GRCh37 using the DRAGEN Enrichment App (Illumina, USA), which also performed variant calling for single nucleotide variants (SNVs) and small insertions/deletions. Filtering criteria included exclusion of variants showing strand bias (strand bias score ≠ -100), low allele frequency (<2%), or poor-quality scores. Also, mapping quality threshold (>30) was set to exclude low-confidence reads, thereby reducing the inclusion of sequencing artifacts. Variant annotation and filtering were

performed using ANNOVAR tool with population (e.g., gnomAD) and clinical (e.g., ClinVar) databases and Franklin database to prioritize variants based on frequency and pathogenicity for downstream interpretation.

Univariate survival analysis according to genomic variants

Univariate survival analyses were performed to evaluate the association between individual genomic variants and clinical outcomes, overall survival (OS) and time to progression (TTP). For each variant, patients were stratified into wild-type and mutated groups. Kaplan–Meier survival curves were generated for each comparison, and differences between groups were assessed using the log-rank test. Survival analyses were conducted using R. Multiple testing correction was applied using the Benjamini–Hochberg false discovery rate (FDR) method. Censoring was appropriately handled in all survival analyses, with tick marks on Kaplan–Meier curves indicating censored observations rather than death or progression events. Summary statistics, including log-rank p-values and FDR-adjusted p-values, were systematically exported for downstream interpretation.

Associations between genomic variants and clinical characteristics

Associations between genomic variants and clinical or disease-related categorical variables were evaluated using contingency table–based statistical testing. For each variant, patients were grouped according to mutation status (wild-type vs mutated), and comparisons were performed against clinical variables including MBD status, the Revised International Staging System (R-ISS) at diagnosis, the presence of osteolytic lesions, sex, magnetic resonance imaging (MRI) pattern, and cytogenetic risk category. Given the small sample size, Fisher's exact test was applied for all comparisons. When

numerical variables were present, the appropriate statistical test was automatically selected; however, all variables included in the present analysis were categorical. To account for multiple hypothesis testing, p-values were adjusted using the Benjamini–Hochberg FDR method.

Supplementary tables

Supplementary Table 1*: Baseline NDMM patient characteristics stratified by the presence of MBD. NDMM, newly diagnosed multiple myeloma; MBD, myeloma bone disease; ECOG PS, Eastern Cooperative Oncology Group Performance Status; ISS, International Staging System; R-ISS, Revised International Staging System; WBC, white blood cell count; ANC, absolute neutrophil count; ALP, alkaline phosphatase; LDH, lactate dehydrogenase; HDM-ASCT, high-dose melphalan with autologous stem cell transplantation; IMiD, immunomodulatory drug; PI, proteasome inhibitor; mAb, monoclonal antibody.*

Variable	**MBD (n=46)**	**Absence of MBD (n=25)**	**p-value**
Age – median (years)	65 (49–88)	65 (46–89)	0.995
Female sex – n (%)	26 (54.2)	13 (56.5)	0.715
ECOG PS ≥2 – n (%)	7 (15.2)	3 (12.0)	0.988
ISS – n (%)			**0.026**
1	24 (52.2)	13 (52.0)	
2	10 (21.7)	11 (44.0)	
3	12 (25.0)	1 (4.0)	
R-ISS – n (%)			**0.040**
1	19 (41.3)	8 (32.0)	
2	20 (43.5)	17 (68.0)	

3	7 (15.2)	0 (0.0)	
High-risk cytogenetics – n (%)	20 (43.5)	9 (36.0)	0.925
Osteolytic lesions – n (%)			
1–3	19 (41.3)	–	
4–10	8 (17.4)	–	
>10	19 (41.3)	–	
Hemoglobin (g/dL)	11.3 (6.2–13.4)	11.9 (8.6–15.0)	0.964
WBC ($\times 10^9$/L)	5.5 (0.7–16.5)	6.4 (2.7–10.4)	0.393
ANC ($\times 10^9$/L)	3.0 (1.2–13.8)	3.4 (1.4–7.6)	0.620
Platelets ($\times 10^9$/L)	239 (138–425)	231 (15–708)	0.426
Urea (mg/dL)	37 (20–69)	36 (14–65)	0.953
Albumin (g/dL)	3.9 (2.9–4.8)	3.8 (3.0–4.7)	0.680
Creatinine (mg/dL)	0.8 (0.5–2.5)	0.9 (0.5–1.9)	0.973
ALP (IU/L)	66 (36–184)	57 (27–177)	0.457
Calcium (mg/dL)	9.4 (8.2–13.3)	9.2 (8.2–10.4)	0.312
Bone marrow infiltration (%)	40 (4–100)	60 (12–95)	0.127
Serum β2-microglobulin (mg/L)	3.2 (1.2–15.0)	2.7 (1.4–5.9)	0.400
LDH (IU/L)	164 (60–309)	143 (101–1692)	0.303
Heavy chain type – n (%)			0.979

IgG	33 (71.7)	18 (72.0)	
IgA	11 (23.9)	6 (24.0)	
Light chain only	2 (4.3)	1 (4.0)	
Light chain type – n (%)			0.142
κ	32 (69.6)	13 (52.0)	
λ	14 (30.4)	12 (48.0)	
M-protein (g/dL)	2.9 (0.0–5.7)	2.8 (0.0–6.6)	0.761
IgG (mg/dL)	2055 (208–7210)	1605 (3–9290)	0.998
IgA (mg/dL)	58 (22–5160)	82 (22–4820)	0.579
IgM (mg/dL)	20 (11–199)	20 (17–81)	0.794
HDM-ASCT – n (%)	11 (23.9)	6 (24.0)	0.547
Treatment – n (%)			0.544
IMiD-based	1 (2.2)	2 (8.0)	
PI + IMiD	17 (37.0)	7 (28.0)	
mAb-based	25 (54.4)	15 (60.0)	
Chemotherapy	3 (6.5)	1 (4.0)	

Supplementary Table 2: *Statistical analysis for clinical outcomes for the circulating markers quantified by ELISA or LEGENDplex in newly diagnosed multiple myeloma patients.CI: confidence interval; HR: Hazard ratio*

A. ELISA															
Protein	**Endpoint**	**Optimal cutoff**	**Median survival (low)**	**Median survival (High)**	**Log-rank p**	**Univariable HR**	**Univariable 95% CI (Lower)**	**Univariable 95% CI (Upper)**	**Univariable p**	**Multivariable HR**	**Multivariable 95% CI (Lower)**	**Multivariable 95% CI (Upper)**	**Multivariable p**	**Adjusted log-rank p**	**Adjusted univariable p**
Sema D	PFS	12.29	1435.00	502.00	0.01	2.76	1.23	6.18	0.01	3.03	1.06	8.66	0.04	0.04	0.06
Sema D	TTP	13.15		588.50	0.03	2.95	1.06	8.22	0.04	3.62	0.99	13.29	0.05	0.06	0.09
Periostin	TTP	196.78	816.00		0.04	0.36	0.13	0.99	0.05	0.38	0.12	1.15	0.09	0.07	0.10
Periostin	PFS	196.78	816.00		0.23	0.61	0.27	1.38	0.24	0.45	0.17	1.22	0.12	0.24	0.29
Activin A	PFS	170.62	842.00		0.16	0.26	0.04	1.94	0.19	0.27	0.03	2.18	0.22	0.19	0.24
Activin A	TTP	100.68	1435.00		0.13	0.24	0.03	1.81	0.17	0.28	0.03	2.32	0.24	0.17	0.23
Periostin	OS	545.45		1788.00	0.00	6.02	1.60	22.66	0.01	0.60	0.07	5.32	0.64	0.02	0.05
Activin A	OS	34.53			0.22	3.41	0.42	27.76	0.25	1.52	0.16	14.48	0.72	0.24	0.30
Sema D	OS	13.15			0.20	0.00	0.00	Inf	1.00	0.00	0.00	Inf	1.00	0.22	1.00
B. Multiplate Analysis															
Protein	**Endpoint**	**Optimal cutoff**	**Median survival (low)**	**Median survival (High)**	**Log-rank p**	**Univariable HR**	**Univariable 95% CI (Lower)**	**Univariable 95% CI (Upper)**	**Univariable p**	**Multivariable HR**	**Multivariable 95% CI (Lower)**	**Multivariable 95% CI (Upper)**	**Multivariable p**	**Adjusted log-rank p**	**Adjusted univariable p**
ACP5	TTP	5203.20	885.00		0.02	0.25	0.07	0.85	0.03	0.16	0.04	0.59	0.01	0.10	0.23
DKK-1	TTP	1868.70	885.00	1435.00	0.07	0.37	0.12	1.11	0.08	0.24	0.07	0.86	0.03	0.16	0.28
OPG	OS	3996.61			0.01	5.08	1.38	18.75	0.01	10.82	1.29	90.65	0.03	0.07	0.21
RANKL	PFS	331.19		775.00	0.14	1.97	0.79	4.90	0.14	4.53	1.13	18.08	0.03	0.19	0.28
IL-1β	PFS	3.35		675.00	0.00	5.18	1.81	14.87	0.00	5.55	1.14	27.03	0.03	0.02	0.11
ACP5	PFS	5203.20	791.00		0.09	0.48	0.20	1.15	0.10	0.37	0.14	0.99	0.05	0.19	0.28

Supplementary Table 3: *Statistical comparison of circulating bone metabolism markers measured by the LEGENDplex™ Human Bone Metabolism Panel between patients with and without multiple myeloma–related bone disease (MBD) using the Mann–Whitney U test. ACP5, Acid Phosphatase 5; ALPL, Alkaline Phosphatase; DKK-1, Dickkopf-related Protein 1; IL-1β, Interleukin-1 beta; IL-6, Interleukin-6; OPG, Osteoprotegerin; OPN, Osteopontin; PDGF-BB, Platelet-Derived Growth Factor BB; PTH, Parathyroid Hormone; RANKL, Receptor Activator of Nuclear Factor Kappa-B Ligand; TNF-α, Tumor Necrosis Factor alpha.*

Protein	**P_value**	**Adj_P_value**
ACP5	0.228	0.448
ALPL	0.522	0.679
DKK-1	0.062	0.401
IL-1β	0.566	0.679
IL-6	0.125	0.401
Leptin	0.243	0.448
OPG	0.555	0.679
OPN	0.150	0.401
PDGF-BB	0.236	0.448
PTH	0.143	0.401
RANKL	0.626	0.715
TNF-α	0.740	0.808

Supplementary Table 4: *Association of circulating bone metabolism markers with the presence of osteolytic lesions across disease stages (SMM/MGUS and NDMM). ACP5, Acid Phosphatase 5; ALPL, Alkaline Phosphatase; DKK-1, Dickkopf-related Protein 1; IL-1β, Interleukin-1 beta; IL-6, Interleukin-6; OPG, Osteoprotegerin; OPN, Osteopontin; PDGF-BB, Platelet-Derived Growth Factor BB; PTH, Parathyroid Hormone; RANKL, Receptor Activator of Nuclear Factor Kappa-B Ligand; TNF-α, Tumor Necrosis Factor alpha.*

Protein	**P_value**	**Adj_P_value**
ACP5	0.283	0.796
ALPL	0.747	0.833
DKK-1	0.727	0.833
IL-1β	0.764	0.833
IL-6	0.244	0.796
Leptin	0.532	0.796
OPG	0.078	0.796
OPN	0.153	0.796
PDGF-BB	0.394	0.796
PTH	0.287	0.796
RANKL	0.490	0.796
TNF-α	0.741	0.833

Supplementary Table 5: *Statistical comparison of circulating markers between patients with and without multiple myeloma–related bone disease (MBD) using the Mann–Whitney U test. L1TD1, LINE-1 Type Transposase Domain Containing 1; SHTN1, Shootin 1; MYH16, Myosin Heavy Chain 16; GIGYF2, GRB10 Interacting GYF Protein 2; B2M, Beta-2-Microglobulin; ARFGEF3, ADP-Ribosylation Factor Guanine Nucleotide Exchange Factor 3; F12, Coagulation Factor XII; AMBP, Alpha-1-Microglobulin/Bikunin Precursor; ARAP3, ArfGAP with RhoGAP Domain, Ankyrin Repeat and PH Domain 3; FHOD1, Formin Homology 2 Domain Containing 1; HSPA1L, Heat Shock Protein Family A (Hsp70) Member 1 Like.*

Protein	**P_value**	**Adj_P_value**
L1TD1	0.0005	0.13861
SHTN1	0.0021	0.31573
MYH16	0.0093	0.70729
GIGYF2	0.0094	0.70729
B2M	0.0147	0.88619
ARFGEF3	0.0227	1.00000
F12	0.0268	1.00000
AMBP	0.0282	1.00000
ARAP3	0.0348	1.00000
FHOD1	0.0358	1.00000
HSPA1L	0.0440	1.00000

Supplementary figures

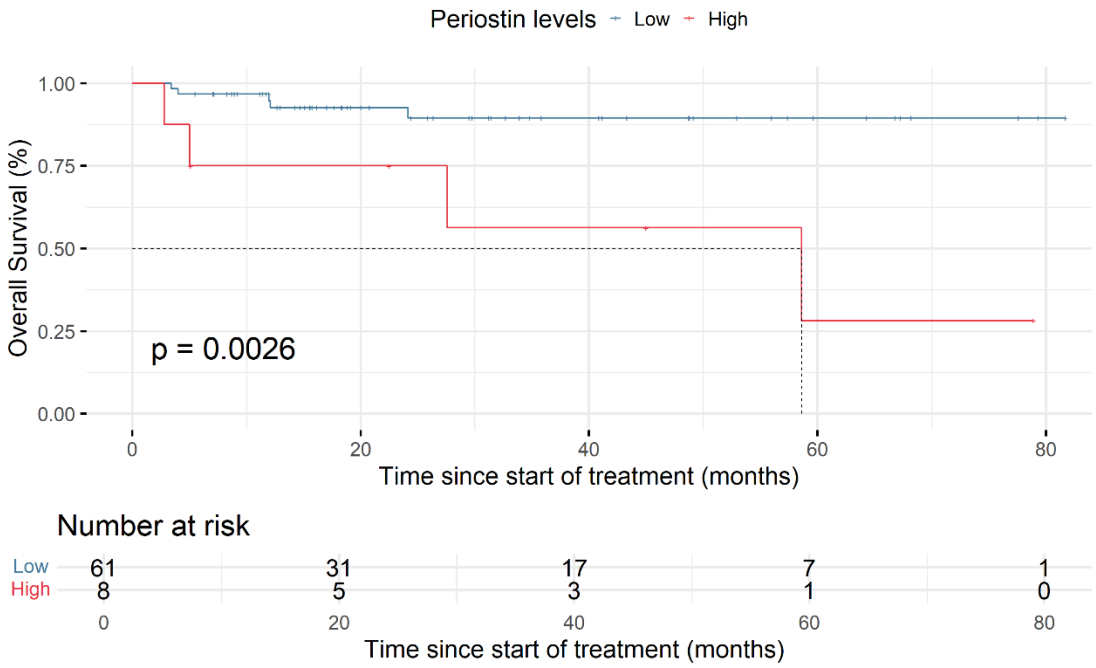

Supplementary Figure 1. Univariate Kaplan–Meier survival analysis according to periostin levels in newly diagnosed multiple myeloma (NDMM) patients. Kaplan–Meier curve for overall survival (OS) stratified by periostin levels (high vs low). Patients were dichotomized based on an optimal cutoff value which was defined via maximal ranked statistics. Survival differences between groups were evaluated using the log-rank test.

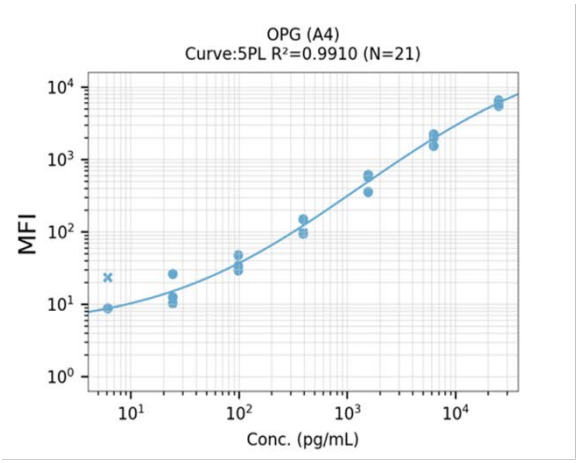
OPG (A4)
Curve:5PL R²=0.9910 (N=21)
MFI
Conc. (pg/mL)

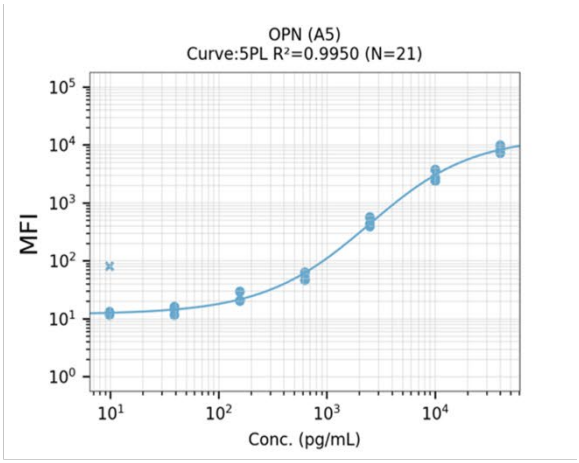
OPN (A5)
Curve:5PL R²=0.9950 (N=21)
MFI
Conc. (pg/mL)

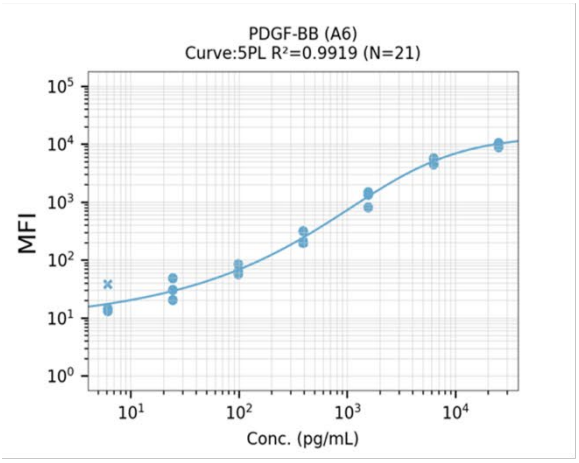
PDGF-BB (A6)
Curve:5PL R²=0.9919 (N=21)
MFI
Conc. (pg/mL)

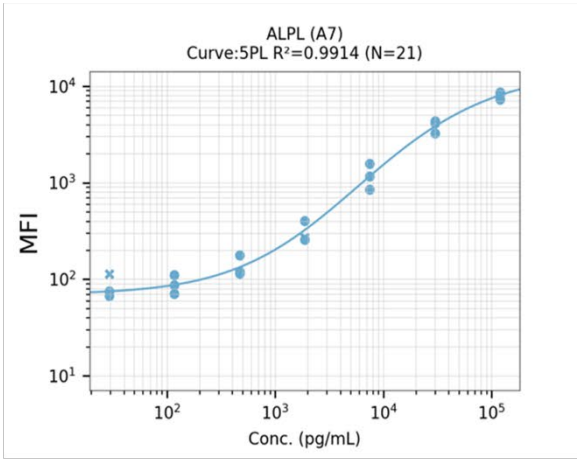
ALPL (A7)
Curve:5PL R²=0.9914 (N=21)
MFI
Conc. (pg/mL)

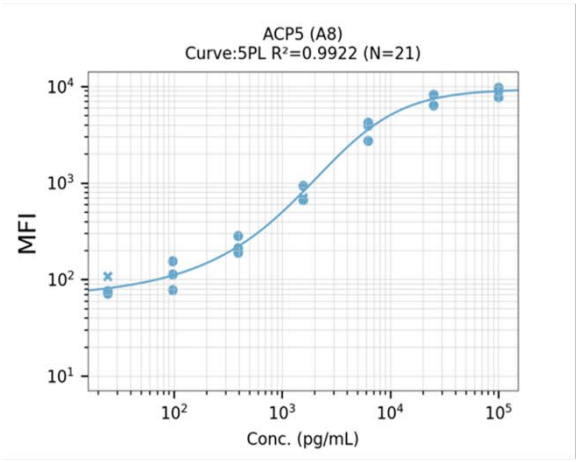
ACP5 (A8)
Curve:5PL R²=0.9922 (N=21)
MFI
Conc. (pg/mL)

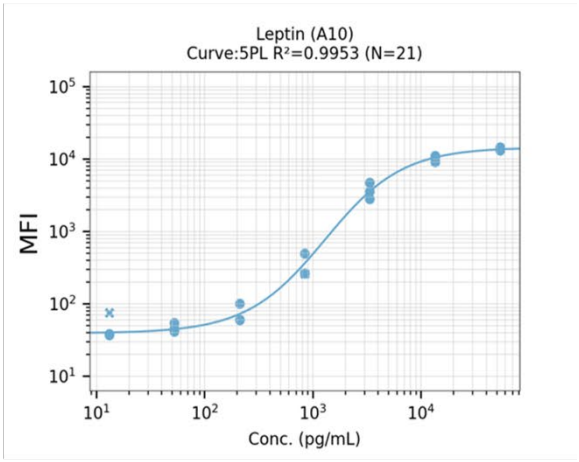
Leptin (A10)
Curve:5PL R²=0.9953 (N=21)
MFI
Conc. (pg/mL)

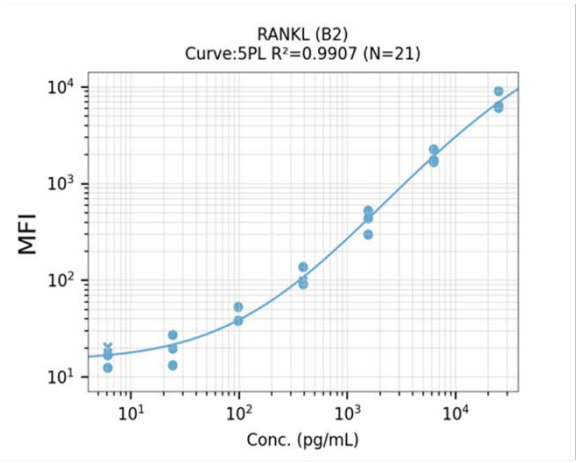
RANKL (B2)
Curve:5PL R²=0.9907 (N=21)
MFI
Conc. (pg/mL)

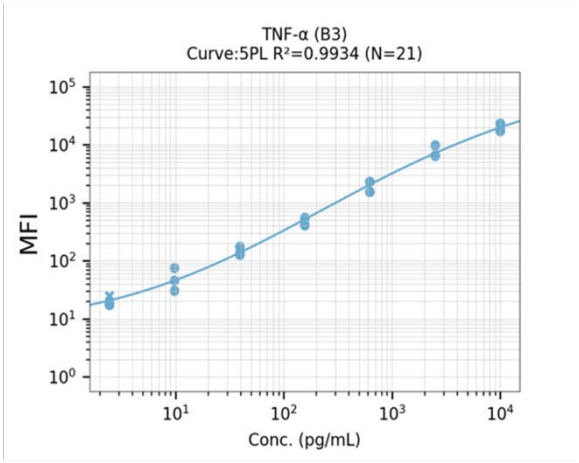
TNF-α (B3)
Curve:5PL R²=0.9934 (N=21)
MFI
Conc. (pg/mL)

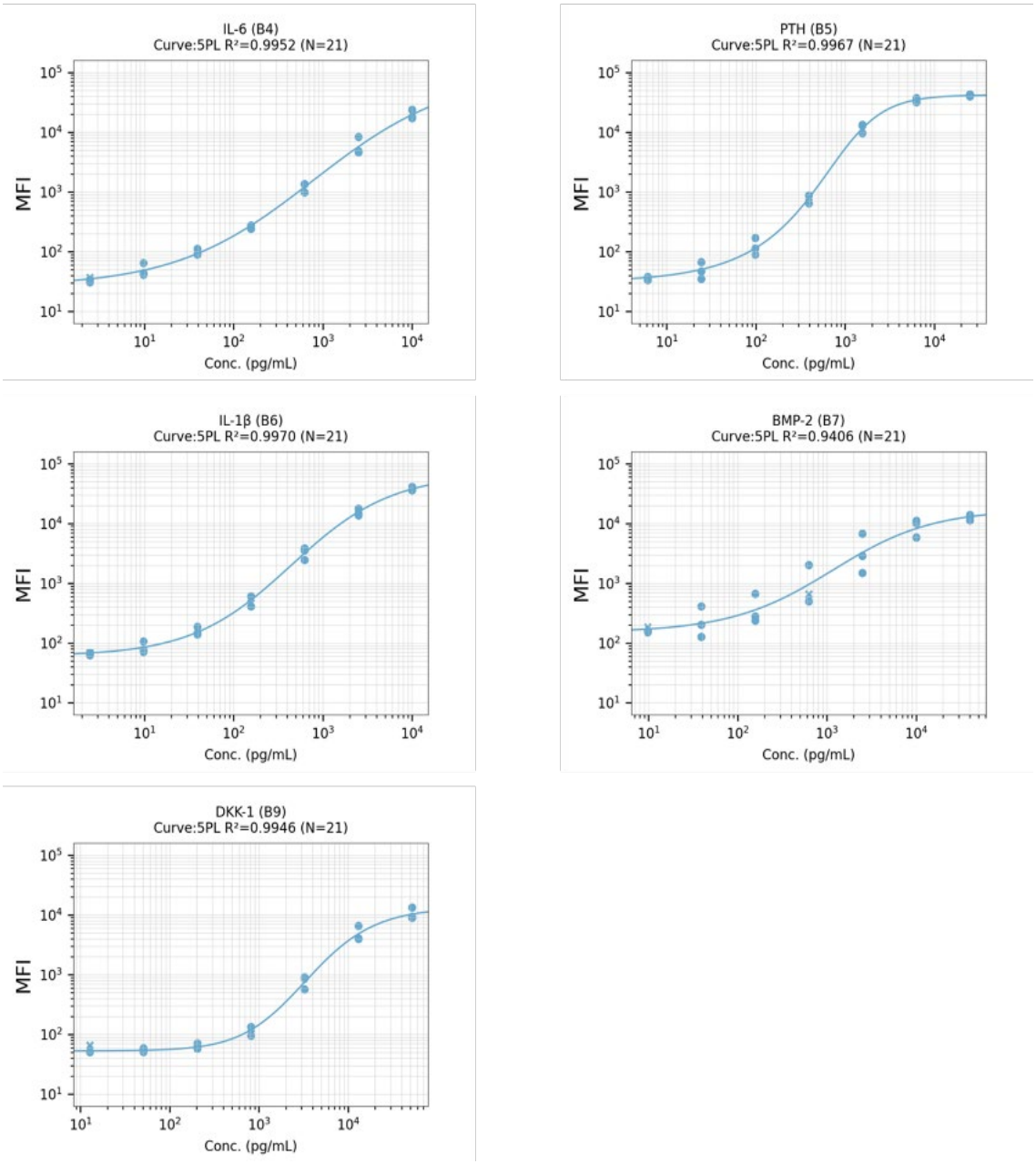

Supplementary Figure 2. Standard curves of the LEGENDplex™ Human Bone Metabolism Panel. *Representative standard curves generated for the quantitative determination of bone metabolism–related analytes using the LEGENDplex™ Human Bone Metabolism multiplex assay. Standard curves were constructed for osteoprotegerin (OPG), osteopontin (OPN), platelet-derived growth factor-BB (PDGF-BB), alkaline phosphatase (ALPL), tartrate-resistant acid phosphatase 5 (ACP5), leptin, receptor activator of nuclear factor-κB ligand (RANKL/TRANCE), tumor necrosis factor-*

α (TNF-α), interleukin-6 (IL-6), parathyroid hormone (PTH), interleukin-1β (IL-1β), bone morphogenetic protein-2 (BMP-2), and Dickkopf-1 (DKK-1). Serial dilutions of assay standards were analyzed according to the manufacturer's instructions, and mean fluorescence intensity (MFI) was plotted against known analyte concentrations. Curves were generated using a five-parameter logistic (5-PL) regression model and were used for the calculation of analyte concentrations in experimental samples.

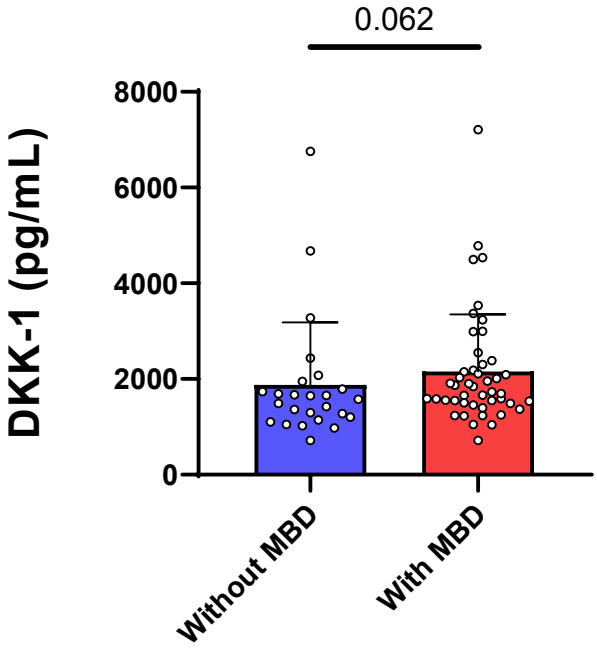

Supplementary Figure 3. Alterations in circulating bone metabolism–related markers associated with myeloma bone disease (MBD). *Circulating levels of Dickkopf-related protein 1 (DKK-1) in the NDMM patients. Mann–Whitney U test between patients with and without MBD.*

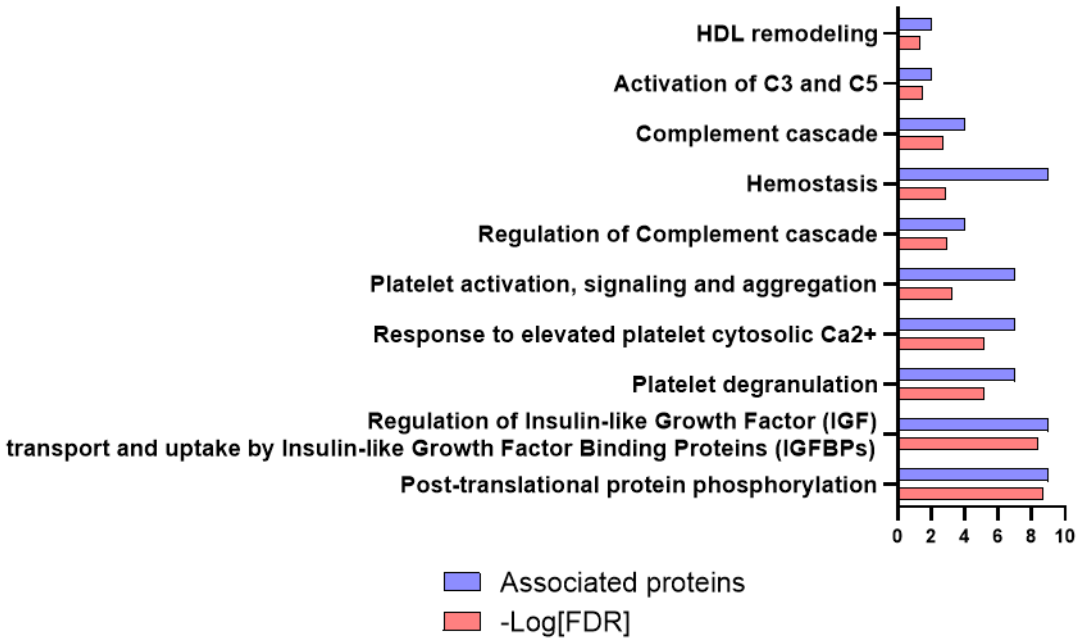

Supplementary Figure 4. *Reactome pathway enrichment analysis of proteins associated with the number of osteolytic lesions per patient. Although these proteins showed nominal significance, they did not remain significant after false discovery rate (FDR) correction. Enrichment analysis was conducted using WebGestalt.*

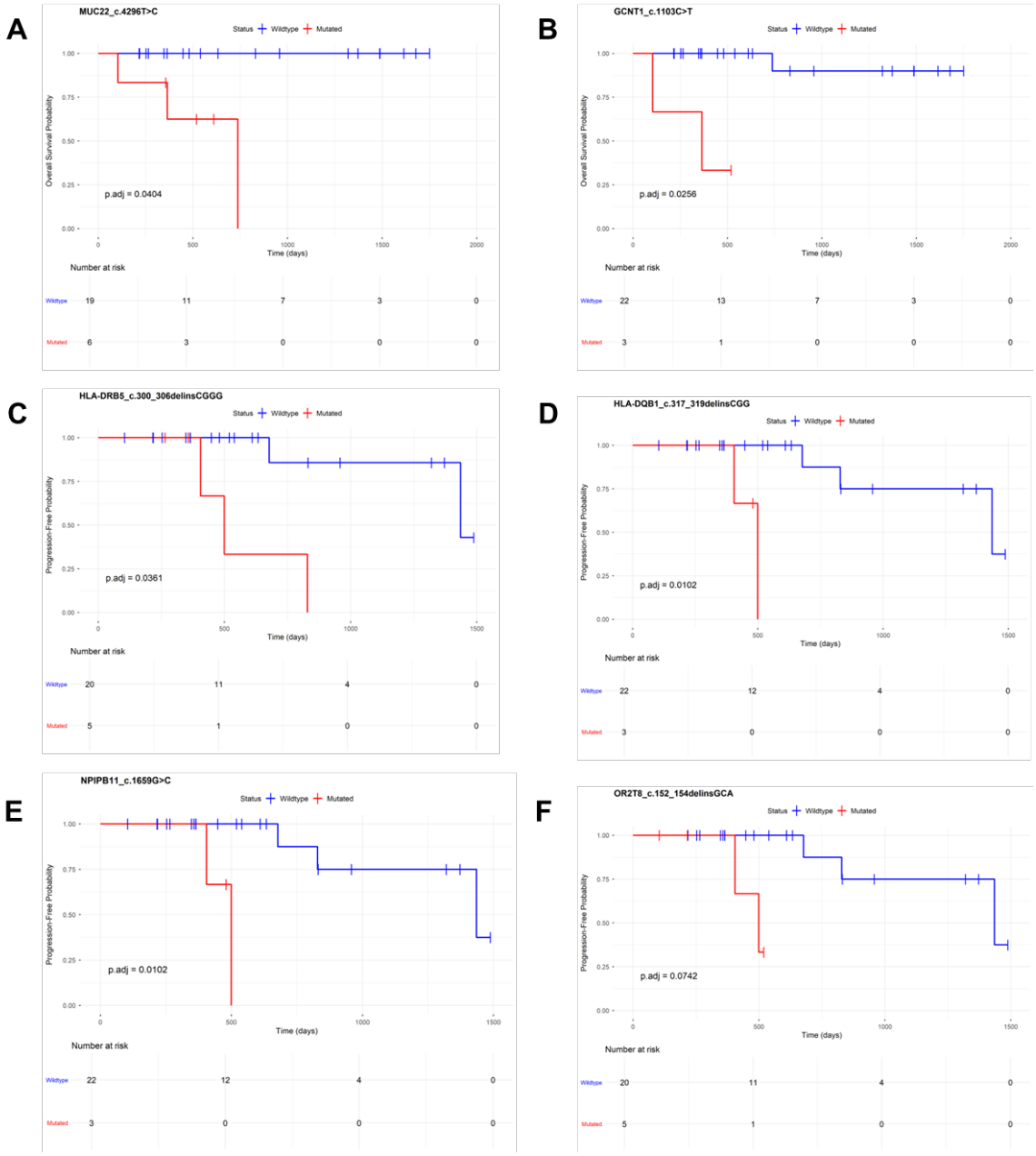

Supplementary Figure 5. Kaplan–Meier survival analysis for genomic variants associated with clinical outcomes. *(A, B) Overall survival (OS) curves for patients carrying the MUC22 c.4296T>C (synonymous, possibly benign, non-somatic) and GCNT1 c.1103C>T (non-synonymous, possibly benign, somatic) variants, which remained significantly associated with OS following adjustment for multiple testing. (C, D) Time to progression (TTP) curves for variants in HLA class II genes: HLA-DRB5 c.300_306delinsCGGG (non-frameshift, possibly pathogenic, non-somatic) and HLA-*

DQB1 c.317_319delinsCGG (non-synonymous, of uncertain significance, somatic), associated with inferior TTP. (E, F) TTP curves for additional variants associated with worse outcomes: NPIPB11 c.1659G>C (synonymous, likely benign, non-somatic) and OR2T8 c.152_154delinsGCA (non-synonymous, of uncertain significance, somatic).

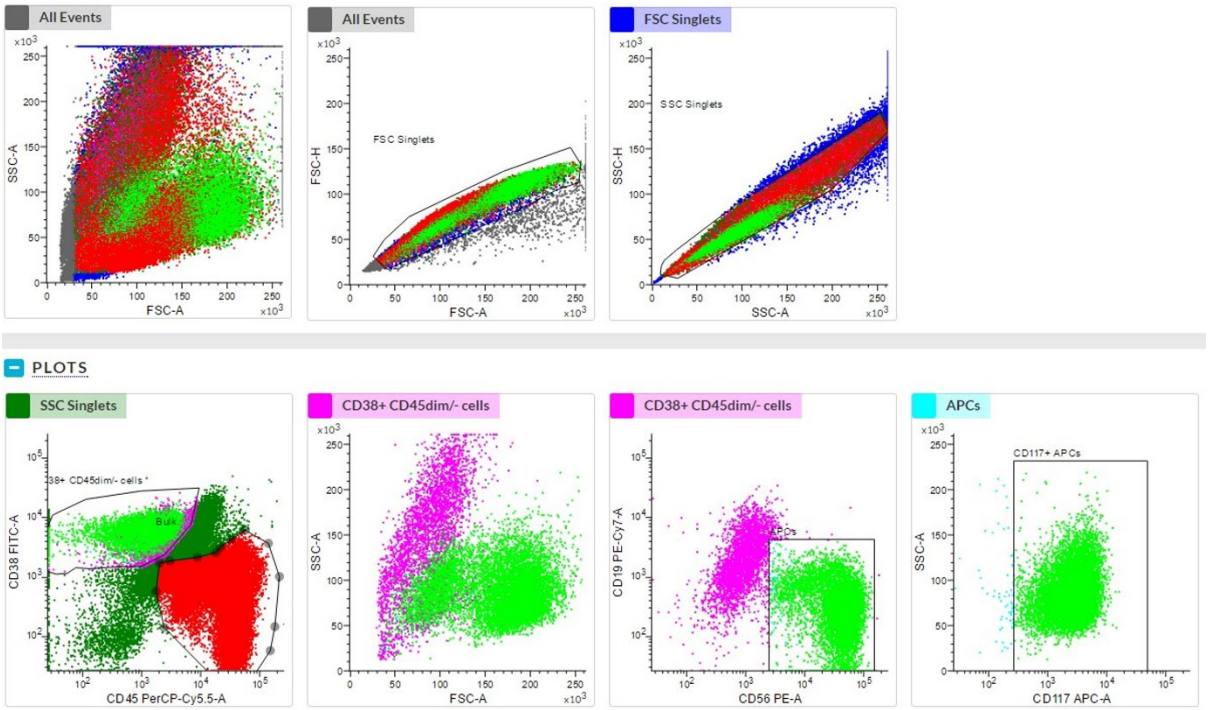

Supplementary Figure 6: *Gating strategy for the sorting of clonal cells from cryopreserved bone marrow nucleated cells. Gated cells in green are an example of the selected clonal plasma cells, while gated cells in red are the bulk population of the bone marrow. APCs, aberrant plasma cells.*

References

1. Nikolaou PE, Mylonas N, Makridakis M, et al. Cardioprotection by selective SGLT-2 inhibitors in a non-diabetic mouse model of myocardial ischemia/reperfusion injury: a class or a drug effect? *Basic Res Cardiol*. 2022;117(1):27. doi:10.1007/s00395-022-00934-7

2. Efentakis P, Lamprou S, Makridakis M, et al. Mineralocorticoid Receptor Pathway Is a Key Mediator of Carfilzomib-induced Nephrotoxicity: Preventive Role of Eplerenone. *Hemasphere*. 2022;6(11):e791. doi:10.1097/HS9.0000000000000791

3. Nikolaou PE, Efentakis P, Abu Qourah F, et al. Chronic Empagliflozin Treatment Reduces Myocardial Infarct Size in Nondiabetic Mice Through STAT-3-Mediated Protection on Microvascular Endothelial Cells and Reduction of Oxidative Stress. *Antioxid Redox Signal*. 2021;34(7):551-571. doi:10.1089/ars.2019.7923

4. Nikolaou PE, Mylonas N, Makridakis M, et al. Cardioprotection by selective SGLT-2 inhibitors in a non-diabetic mouse model of myocardial ischemia/reperfusion injury: a class or a drug effect? *Basic Res Cardiol*. 2022;117(1):27. doi:10.1007/s00395-022-00934-7

5. Mokou M, Klein J, Makridakis M, et al. Proteomics based identification of KDM5 histone demethylases associated with cardiovascular disease. *EBioMedicine*. 2019;41:91-104. doi:10.1016/j.ebiom.2019.02.040

6. Lygirou V, Latosinska A, Makridakis M, et al. Plasma proteomic analysis reveals altered protein abundances in cardiovascular disease. *J Transl Med*. 2018;16(1):104. doi:10.1186/s12967-018-1476-9

7. Stroggilos R, Mokou M, Latosinska A, et al. Proteome-based classification of Nonmuscle Invasive Bladder Cancer. *Int J Cancer*. Published online July 8, 2019. doi:10.1002/ijc.32556

8. Margelos T, Makridakis M, Gonidaki C, et al. Simple, Fast, and Reliable Analysis of Label-Free Proteomics Data With the Proteomics Eye (ProtE). *PROTEOMICS – Clinical Applications*. 2026;20(1):e70037. doi:10.1002/prca.70037

9. Wang J, Vasaikar S, Shi Z, Greer M, Zhang B. WebGestalt 2017: a more comprehensive, powerful, flexible and interactive gene set enrichment analysis toolkit. *Nucleic Acids Res*. 2017;45(W1):W130-W137. doi:10.1093/nar/gkx356

10. Liao Y, Wang J, Jaehnig EJ, Shi Z, Zhang B. WebGestalt 2019: gene set analysis toolkit with revamped UIs and APIs. *Nucleic Acids Research*. 2019;47(W1):W199-W205. doi:10.1093/nar/gkz401